THE JOURNAL OF PHYSICAL CHEMISTRY B

Article

pubs.acs.org/JPCB

pH-Independence of Trialanine and the Effects of Termini Blocking in Short Peptides: A Combined Vibrational, NMR, UVCD, and Molecular Dynamics Study

Siobhan Toal,[†] Derya Meral,[‡] Daniel Verbaro,[†,§] Brigita Urbanc,[‡] and Reinhard Schweitzer-Stenner*[,†]

[†]Departments of Chemistry, [§]Biology and [‡]Physics, Drexel University, 3141 Chestnut Street, Philadelphia, Pennsylvania 19104, United States

Supporting Information

ABSTRACT: Several lines of evidence now well establish that unfolded peptides in general, and alanine in specific, have an intrinsic preference for the polyproline II (pPII) conformation. Investigation of local order in the unfolded state is, however, complicated by experimental limitations and the inherent dynamics of the system, which has in some cases yielded inconsistent results from different types of experiments. One method of studying these systems is the use of short model peptides, and specifically short alanine peptides, known for predominantly sampling pPII structure in aqueous solution. Recently, He et al. (*J. Am. Chem. Soc.* **2012**, *134*, 1571−1576) proposed that unblocked tripeptides may not be suitable models for studying conformational propensities in unfolded peptides due to the presence of end effect, that is, electrostatic interactions between investigated amino acid residues and terminal charges. To determine whether changing the protonation states of the N- and C-termini influence the conformational manifold of the central amino acid residue in tripeptides, we have examined the pH-dependence of unblocked trialanine and the conformational preferences of alanine in the alanine dipeptide. To this end, we measured and globally analyzed amide I′ band profiles and NMR J-coupling constants. We described conformational distributions as the superposition of two-dimensional Gaussian distributions assignable to specific subspaces of the Ramachandran plot. Results show that the conformational ensemble of trialanine as a whole, and the pPII content (χ_{pPII} = 0.84) in particular, remains practically unaffected by changing the protonation state. We found that compared to trialanine, the alanine dipeptide has slightly lower pPII content (χ_{pPII} = 0.74) and an ensemble more reminiscent of the unblocked Gly-Ala-Gly model peptide. In addition, a two-state thermodynamic analysis of the conformational sensitive $\Delta\varepsilon(T)$ and $^3J(H^NH^\alpha)(T)$ data obtained from electronic circular dichroism and H NMR spectra indicate that the free energy landscape of trialanine is similar in all protonation states. MD simulations for the investigated peptides corroborate this notion and show further that the hydration shell around unblocked trialanine is unaffected by the protonation/deprotonation of the C-terminal group. In contrast, the alanine dipeptide shows a reduced water density around the central residue as well as a less ordered hydration shell, which decreases the pPII propensity and reduces the lifetime of sampled conformations.

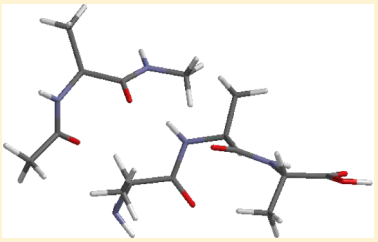

INTRODUCTION

Short unfolded peptides have emerged as suitable model systems for determining the conformational propensities of amino acids in aqueous solution.[1−16] From an analysis of the conformational space sampled by blocked dipeptides, Tanford, Ramachandran and Flory described the unfolded state of peptides and proteins alike as a random coil with a nearly sequence independent conformational distribution.[17−19] Over the last 20 years, however, multiple experimental, and in part even theoretical, evidence has been provided for the notion that the conformational space of most amino acid residues is much more restricted than suggested by the random coil model.[3−5,10−12,20−22] Moreover, it has become clear that amino acid residues show different conformational distributions, which can be altered by the nearest neighbors.[3,22−26] In this context, polyproline II (pPII) has emerged as the dominant conformation for alanine,[10] whereas the pPII propensity of other residues is still a matter of controversial debate.[3,10,11,27] The canonical pPII conformation with $(\varphi,\psi) = (-75°, 150°)$ is adopted by residues in *trans*-polyproline where it brings about a 3_1-helix structure of the peptide.

Over the last 10 years, different types of short peptides have been used to explore the conformational propensities of amino acids in the unfolded state. The appropriate choice of model peptides is being debated. Blocked dipeptides are often considered as an ideal choice, owing to the absence of any terminal charges which are thought to affect the conformation of residues in corresponding unblocked tripeptide systems. With respect to alanine, the alanine dipeptide, Ac-Ala-NHMe, has been the classical model system particularly for computational studies of alanine conformations.[8,13,14,18,19,28−40] Nearly 50 years after Ramachandran, Flory and co-workers used this peptide[18,19] as a kind of canonical model system for describing the Ramachandran plot of residues in the unfolded state, numerous MD studies still use this peptide to explore the underlying physics of the pPII preference of alanine.[29,30,32,36−38,41,42] Several experimental studies (IR, Raman, NMR) on this peptide have been carried out as well.[13,15,33−35,43] Avbelj and co-workers reported propensity scales for all 19 nonproline residues in blocked dipeptides based on an analysis of the amide III region of their Raman and IR spectra.[13,34,35] Oh et al. used NMR and CD spectroscopy to analyze the

Received: October 22, 2012
Revised: February 27, 2013
Published: February 28, 2013

conformational properties of 361 blocked tripeptides.[44,45] In contrast, other researchers used unblocked peptides like trialanine (AAA) and GxG (x: different guest amino acid residues) for conformational studies, in part because these types of peptides allow more comprehensive NMR studies and provide a better spectral resolution in the amide I window of vibrational spectra, which is a highly prominent tool for the structure analysis of peptides and proteins alike.[5−7,10,11,46−50] The choice of unblocked tripeptides was justified with experimental evidence for the limited influence of terminal charges on the conformation of their central residues.[10,48] Recently, however, Kallenbach and co-workers launched a major criticism of the use of tripeptides for conformational studies.[27] They cite the fact that four guest residues in GxG, AcGxGNH2, and AcGGxGGNH2, and the respective dipeptides show slightly different $^3J(H^NH^\alpha)$ coupling constants at different pH as an argument for the influence of terminal groups. Using a two-state analysis of ^3J coupling data along with reference J_{pPII} and J_β values obtained from pPII/β maxima in coil libraries,[51,52] they obtained an increase in pPII content along the series (GxG)<(AcGxGNH$_2$)<(AcGGxGGNH$_2$). This analysis led them to conclude that the free terminal groups of, for example, GxG cause a 15% reduction of pPII propensities of the central residue and that blocked dipeptides or even blocked glycine-based host−guest systems would be more appropriate model systems. However, caution has to be taken when analyzing $^3J(H^NH^\alpha)$ constants because the observed differences between corresponding GxG, AcGxGNH$_2$ and AcGGxGGNH$_2$ coupling constants could well arise from small shifts of conformational distributions in the Ramachandran space. In the present study, we explore the influence of terminal groups on central amino acid residues in short alanine peptides with experimental and computational means. The experimental part involves a combined analysis of NMR coupling constants and amide I′ band profiles of all three protonation states of AAA as well as of the alanine dipeptide (AdP). Thus, we are addressing two questions: (1) To what extent does the protonation state of the terminal groups affect the intrinsic conformational propensity of central amino acid residues in tripeptides with unblocked termini and (2) how does termini blocking (i.e., "capping") affect this conformational propensity? In this context, we are also in a position to address the question of whether or not the heterogeneity of the CO-bonds of peptide groups have to be taken into account explicitly for the modeling of the significantly overlapping amide I bands of anionic AAA and AdP.[38,46,47] In addition to determining the influence of free termini on central alanine residue's conformational distribution at room temperature, we also explore the thermodynamics governing the pPII preference for AdP and AAA in all protonation states by analyzing the temperature dependence of conformationally sensitive CD and NMR parameters. The second, computational part of our investigation utilizes molecular dynamics (MD) simulations. As indicated above the assumed suitability of AdP as the simplest model system for studying peptide conformations has led to a flood of MD studies on this peptide *in vacuo* and in aqueous solution.[8,29,30,32,36−38,40−43] One of the reasons for this multitude of studies is that MD simulations of unfolded peptides heavily depend on the choice of the force field.[53,54] While earlier simulations with CHARMM and AMBER force fields led to an overemphasis of right-handed helical conformations,[21,30,54−56] more recent modified CHARMM and AMBER as well as OPLS force fields yielded a dominant population of the pPII/β conformations in the upper left quadrant of the Ramachandran plot.[57,58] Some advances have recently been made by combining MD simulation for the solvent with DFT calculations for the peptide.[42,50] However, most of these simulations still predicted pPII populations in amounts well below the recently reported experimental values. Exceptions from the rule are strongly modified AMBER and CHARMM force fields, which yielded a rather high fraction of pPII (0.8 and 0.99) for AAA and AdP, respectively.[20,43,56] However, the physical rationale for these changes (i.e., eliminating the torsional potential for φ and ψ in AMBER and a highly polarizable version of CHARMM) remains somewhat obscure. Kwac et al. performed MD simulations of AdP with several normal and polarizable force fields and different water models and found that only the combination of a polarizable AMBER ff02 force field with a polarizable water model yielded pPII fraction slightly higher than 0.5.[43] Here, our experimental studies of AAA and AdP are complemented by MD simulations that combine two force fields with several commonly used water models. The relative validity of the resulting conformational manifolds was validated by comparison to experimentally derived distributions. Moreover, the MD simulations revealed some interesting insights about difference between the conformational dynamics and hydration shell structures of the investigated peptides.

MATERIAL AND METHODS

Materials. Alanyl-alanyl-alanine (H-Ala-Ala-Ala-OH • acetate) and the alanine dipeptide (CH_3−CONH−$CHCH_3$−CONH−CH_3) were purchased from Bachem with >98% purity. No further purification was carried out. For the vibrational spectroscopy experiments, a peptide concentration of 0.2 M in D_2O (Sigma Aldrich) was prepared. The pD was adjusted with small aliquots of 35 wt % DCl in D_2O (Sigma Aldrich). The pH was measured using an Accumet Research AR50 pH meter with an Accumet probe (Fisher Scientific). For cationic trialanine, a pD value of 2.0 was calculated using the Glasoe and Long method.[59] We used very acidic conditions to facilitate the NMR measurements.

For HNMR measurements, each peptide was dissolved in a solution of 90% H_20/10% D_20 (1% TMS) at a concentration of 0.2 M. For cationic trialanine and the alanine dipeptide, the sample was titrated to a pD value of 2.0. In order to analyze zwitterionic trialanine, the sample was titrated with DCL to a pD value of 5.5. This choice of pD was specifically made to ensure that the peptide was fully ionized and yet the amide signal was still clearly discernible and able to be properly deconvoluted in order to obtain $^3J(H^NH^\alpha)$ constants.

For the ultraviolet circular dichroism measurements (CD), 10 mM trialanine in 100% D_2O was prepared from a 0.2 M stock solution and sequentially titrated using small aliquots of DCl to obtain a pD of 2.0 for the cationic AAA sample, and a pD of 5.5 for the zwitterionic AAA sample. For the AdP, a similar procedure was carried out where 10 mM AdP in 100% D_2O was prepared from a 0.2 M stock solution and titrated with small aliquots of DCl until desired pD of 2.0 was achieved.

EXPERIMENTAL METHODS

Ultraviolet Circular Dichroism. CD spectra were measured on a Jasco J-810 spectropolarimeter (Jasco, Inc.) purged with N_2. The 0.01 M sample was loaded into a 50 μm International Crystals Laboratories (ICL) cell. Spectra were measured between 180 and 300 nm with a 500 nm/min scan speed, a 1 s response time, a 0.05 data pitch, and a 5 nm bandwidth. Spectra were taken from 10 to 85 °C with 5 °C increments using a Peltier controller (model PTC-423S). All spectra were corrected using appropriate background subtraction.

Vibrational Spectroscopy. Infrared absorption and vibrational circular dichroism (VCD) spectra were measured on a

BioTools ChiralIR. 0.2 M AAA was loaded into a 20 μm CaF_2 Biocell (BioTools). A BioTools water-cooled temperature controller was used to maintain a temperature of 25 °C. Spectra were taken with 8 cm^{-1} resolution and a total integration time of 840 min (756 min for VCD and 84 min for IR). All spectra were collected in Grams/AI 7.00 (Thermo Galactic). The absorbance spectrum was corrected with the subtraction of the appropriate background using Multifit.[60]

Polarized Raman spectra were taken on a Renishaw Ramanscope with a confocal Olympus microscope. A Spectra-Physics argon/krypton ion laser was set to 514.5 nm, and the radiation was directed through a backscattering geometry using a notch filter. The sample was placed in a depression well microscope slide. A coverslip was carefully placed on top of the sample to minimize the presence of air bubbles. The microscope was focused past the coverslip and into the sample. Spectra were measured with scan times of 350 s for both parallel and perpendicular polarized light. Five accumulations were collected and averaged for each polarization. Spectra were measured at ambient temperature. Parallel and perpendicular polarized spectra were used to obtain anisotropic and isotropic scattering profiles, respectively.

NMR Spectroscopy. Amide proton $^3J(H^NH^\alpha)$ coupling constants were determined using ^{1}H NMR. The spectra were recorded on a Varian 500 MHz FT-NMR with a 5 mm HCN triple resonance probe. The temperature was controlled using a Varian VT controller, and spectra were taken between 25 and 65 °C in increments of 5 °C. The sample was allowed to equilibrate at every temperature for a couple of minutes before an experiment was started. For zwitterionic AAA and the AdP, the amide proton signals became unresolvable above 35 and 40 °C, respectively. Hence, data above this temperature were not used for the analysis. Each spectrum was collected with 16 scans, and a PRESAT setting was used to suppress the water. The FIDs were analyzed using Mestrec software, which was used to Fourier transform and phase the data. Then the raw data were analyzed in MultiFit. Amide proton signals were decomposed using Voigtian profiles with flexible half-widths. The frequency positions of the peaks of the Voigtian profiles were plotted as a function of temperature, and a linear regression in SigmaPlot was used to fit the data. The equations generated from the fits were used to calculate the coupling constants as a function of temperature, in line with a procedure described in Toal et al.[61]

MD Simulations. Molecular Dynamics simulations were conducted using all-atom MD in explicit water using GROMACS 4.0.7. For the OPLS force-field,[62] we employed the following three water models: TIP3P,[63] SPCE,[64] and TIP4P.[65] For the simulations with Amber 03 forcefield we also used the TIP4P-Ew water model.[65]

For all simulation trajectories, AAA or AdP were immersed in a box of 51 Å that contained 4466 (TIP3P, SPCE) or 4499 (TIP4P, TIP4P-Ew) water molecules. Energy minimization was applied prior to production runs. In production runs, 2 fs time steps were used in combination with the NPT ensemble at T = 300 K using an extension of the Berendsen thermostat that accounts for canonical sampling through velocity rescaling and P = 1 bar.

THEORY

Amide I′ Simulations. Our theoretical approach utilizes the conformational sensitivity of amide I′ vibrational band in IR, VCD and polarized Raman profiles due to excitonic coupling between local amide I′ modes along the peptide backbone.[66] The amide I′ band is so-called in D_2O to distinguish it from the amide I band in pure H_2O.[67] D_2O is typically used as an aqueous solvent in vibrational studies to avoid the overlap with the rather strong IR band of H_2O at 1640 cm^{-1} and vibrational mixing between amide I and H_2O bending modes.[68,69] In what follows we use the term "amide I" if we describe general physical properties of the mode and the formalism used to account for excitonic coupling, whereas the term "amide I′" is used to describe experimentally obtained band profiles of peptides dissolved in D_2O.

Unblocked tripeptides exhibit two amide I modes at different frequency positions owing to the influence of the terminal groups on the force constant of the carbonyl bond.[70,71] In the absence of excitonic coupling the respective IR and Raman intensities are very similar.[6,46,72] Excitonic coupling causes the splitting between the frequencies of the two modes to increase as well as a redistribution of IR and Raman intensities. The extent of these spectra changes depends on the strength of excitonic coupling and hence on the dihedral angles of the central amino acid residue. This brings about the conformational sensitivity of amide I band profiles.[72] The underlying theory of excitonic coupling as well as our formalism used for the simulation of amide I band profiles have been described in detail previously.[66,73] In this context it is sufficient to mention that the (φ,ψ) dependence of amide I and J-coupling constants are accounted for by mathematically describing the mixing of excited vibrational states via excitonic coupling[66,74] and by Karplus relations for J-coupling constants.[50]

In our analysis conformational distributions are described as a superposition of statistically weighted two-dimensional Gaussian subensembles, the central coordinates and halfwidths of which are used as variable parameters for our simulations.[73] We thus avoid using average or representative conformations. The total distribution function is given by

$$f(\varphi,\psi) = \sum_j \frac{\chi_j}{2\pi\sqrt{|\hat{V}_j|}} e^{-0.5\cdot(\vec{\rho}-\vec{\rho}_j^{\,0})^T \hat{V}_j^{-1}\cdot(\vec{\rho}-\vec{\rho}_j^{\,0})} \tag{1}$$

where:

$$\vec{\rho} = \begin{pmatrix} \varphi \\ \psi \end{pmatrix} \tag{2}$$

and

$$V = \begin{pmatrix} \sigma_\varphi^2 & \sigma_{\varphi\psi}^2 \\ \sigma_{\varphi\psi}^2 & \sigma_\psi^2 \end{pmatrix} \tag{3}$$

is the covariance matrix which contains the half−halfwidths along φ and ψ as diagonal elements. The factor χ_j is the mole fraction of the jth subdistribution.

Two-State Thermodynamic Model. To obtain the enthalpic and entropic differences between pPII and β-strand, we employed a global fitting procedure to analyze the temperature dependence of the conformationally sensitive maximum dichroism $\Delta\varepsilon$ (T) and the $^3J(H^NH^\alpha)$(T) constants with a two-state pPII-β model.[25,61] In this analysis, the experimentally measured $^3J(H^NH^\alpha)$ and $\Delta\varepsilon$ values can be expressed in terms of mole-fraction weighted contributions from each conformation. It is important to note that CD spectra provide information on the net conformational populations of pPII and β-strand, whereas the $^3J(H^NH^\alpha)$ values obtained from ^{1}HNMR provide site-specific information regarding the average φ-values of the central and C-terminal residue according to the Karplus relationship.[50,75] Therefore, we can express $\Delta\varepsilon$(T) generally as

$$\Delta\varepsilon = \Delta\varepsilon_{\mathrm{pPII}}\cdot(2\chi_{\mathrm{pPII-pPII}} + \chi_{\mathrm{pPII}-\beta} + \chi_{\beta-\mathrm{pPII}}) + \Delta\varepsilon_\beta\cdot(2\chi_{\beta-\beta} + \chi_{\mathrm{pPII}-\beta} + \chi_{\beta-\mathrm{pPII}}) \tag{4}$$

dx.doi.org/10.1021/jp310466b | J. Phys. Chem. B 2013, 117, 3689−3706

where χ_{i-j} (i,j = pPII, β) are the mole fractions of the four different net peptide conformations that can contribute to the CD signal for a tripeptide, and $\Delta\varepsilon_{pPII}$ and $\Delta\varepsilon_{\beta}$ are the intrinsic dichroism values of a residue in pPII and β-strand, respectively, in units of M^{-1} cm^{-1}. The factor of 2 for $\chi_{pPII-pPII}$ and $\chi_{\beta-\beta}$ is necessary to account for the case where both residues adopt the same conformation and hence contribute twice to the dichroic value. For a tripeptide with two CD active residues (e.g., AAA) the possible peptide conformers are: $\chi_{pPII-pPII}$, $\chi_{pPII-\beta}$, $\chi_{\beta-pPII}$ and $\chi_{\beta-\beta}$, which are reflected in eq 4. However, for a dipeptide (e.g. AdP, Figure 1), although there are still two peptide bonds, there is only one residue with $\Delta\varepsilon$ values that contribute to the CD spectra. Therefore, in the case of AdP, mixed mole fraction terms in eq 4 are set to zero and the equation can be simplified to

$$\Delta\varepsilon = \chi_{pPII}\Delta\varepsilon_{pPII} + \chi_{\beta}\Delta\varepsilon_{\beta} \tag{5}$$

The mole fractions in eqs 4−5 can then be expressed as a function of temperature using Boltzmann factors. For the $\Delta\varepsilon(T)$ of AAA, this yields

$$\Delta\varepsilon(T) = \frac{[\Delta\varepsilon_{pPII}(2 + e^{-\Delta G_1/RT} + e^{-\Delta G_2/RT}) + \Delta\varepsilon_{\beta}(e^{-\Delta G_1/RT} + e^{-\Delta G_2/RT} + e^{-(\Delta G_1+\Delta G_2)/RT})]}{1 + e^{-\Delta G_1/RT} + e^{-\Delta G_2/RT} + e^{-(\Delta G_1+\Delta G_2)/RT}} \tag{6}$$

where $\Delta G_i = G_{\beta,i} - G_{pPII,i}$ denotes the Gibbs energy difference between pPII and the β-strand conformations of the ith CD-contributing residue, with $i = 1$ denoting the central and $i = 2$ denoting the C-terminal residue. For AdP, eq 7 can be reduced to

$$\Delta\varepsilon(T) = \frac{\Delta\varepsilon_{pPII} + \Delta\varepsilon e^{-\Delta G/RT}}{1 + e^{-\Delta G/RT}} \tag{7}$$

When analyzing ^{1}HNMR data with a two state pPII↔β model, mixed terms are entirely unnecessary as the $^3J(H^NH^{\alpha})$ coupling constant is site specific for the ith amide proton, where we denote $i = 1$ for the amide associated with the central residue and $i = 2$ for the C-terminal amide.

$$^3J_i = \chi_{i,pPII}\,^3J_{i,pPII} + \chi_{i,\beta}\,^3J_{i,\beta} \tag{8}$$

The corresponding algorithm for the temperature dependence of $^3J(H^NH^{\alpha})$ can be written as:

$$^3J_i(T) = \frac{^3J_{i,pPII} + {}^3J_{i,\beta}e^{-\Delta G_i/RT}}{1 + e^{-\Delta G_i/RT}} \tag{9}$$

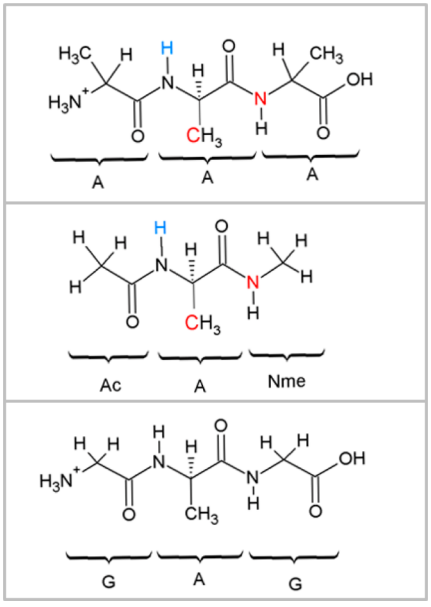

Figure 1. Cationic AAA (upper panel), AdP (middle panel), and cationic GAG peptide (lower panel). Atoms depicted in red were those used in radial distribution function calculations g(r), while those depicted in blue were monitored for distance as a function of the dihedral angle φ (see Figure 10 A−C).

To obtain reference values for $^3J_{pPII}$ and $^3J_{\beta}$ to be used in eq 9, we again use the unique pPII and β-strand subdistributions obtained from vibrational analysis to describe the two substates statistically for each peptide. These distribution functions can be subsequently used to calculate $\langle^3J_{pPII}\rangle$ and $\langle^3J_{\beta}\rangle$ expectation values via the newest version of the Karplus equation.[50]

These reference coupling constants can then be used to calculate the average Gibbs free energy difference between pPII and β-strand substates by employing:

$$\Delta G_i = -RT \cdot \ln\left(\frac{\chi_{\beta,i}}{\chi_{pPII,i}}\right) \tag{10}$$

This can be used to relate ΔH_i and ΔS_i through:

$$\Delta S_i = \frac{\Delta H_i - \Delta G_i(T_R)}{T_R} \tag{11}$$

so that

$$\Delta G_i = \Delta H_i\left(1 - \frac{T}{T_R}\right) + \Delta G_i(T_R) \tag{12}$$

was obtained as the equation to be finally inserted into eq 9 to fit $^3J(H^N,H^{\alpha})(T)$, thus using ΔH_i as the only free parameter.

RESULTS AND DISCUSSION

Early studies on amide I′ band profiles of the isotropic Raman, anisotropic Raman, FT-IR and VCD spectra of all protonation states of AAA in D_2O have been reported by us before.[49,76] In a first attempt we analyzed these profiles in terms of a discrete "representative conformation" which was located between pPII and β-strand regions of the Ramachandran plot. No significant differences between the three protonation states of AAA had emerged from this study.[49] Later, we extended our theoretical approach to consider three representative conformations, that is, pPII, β-strand, and right-handed helical-like conformational subensembles, and utilized the conformationally sensitive $^3J(H^NH^{\alpha})$ constant of the N-terminal amide proton as a fitting restraint.[77,78] This analysis yielded a dominance of pPII conformations (≈50%) with nearly equal admixtures from β-strand and right-handed helical-like conformations. In a more sophisticated study, we analyzed the amide I′ profiles of zwitterionic AAA and a set of six J-coupling constants of cationic AAA reported by Graf et al.[50] using a more realistic distribution model, which describes the conformational ensemble of the central alanine residue in terms of a set of subdistributions associated with pPII, β-strand, right-handed

dx.doi.org/10.1021/jp310466b | J. Phys. Chem. B 2013, 117, 3689−3706

helical and γ-turn like conformations.[73] Each of these subdistributions was described by a two-dimensional normalized Gaussian function. For this analysis we assumed that conformational differences between cationic and zwitterionic AAA are negligibly small. This type of analysis revealed a large pPII fraction of 0.84, in agreement with other experimental results.[1] The discrepancy in pPII content emerging from these different levels of analysis originates from the extreme conformational sensitivity of excitonic coupling between amide I′ modes in the pPII region of the Ramachandran plot. It has become clear that the influence of this coupling is generally not appropriately accounted for by describing the pPII substate by one average or representative conformation. Rather, real statistical models are needed which account for the breadth of each subdistribution. In the study we describe herein, we stick to this type of distribution model (see Sec. Theory) for simulating the amide I′ band profiles of all investigated peptides.

The recent results of He et al.[27] prompted us to closely investigate the pH-dependence of the central residue's conformation in AAA and the corresponding AdP. To this end, we measured the IR and VCD amide I′ profiles of all three protonation states of AAA in D_2O in order to ensure a consistent scaling of respective profiles. In earlier studies of Eker et al., IR and VCD profiles had been measured with different instruments in different laboratories.[49] The Raman band profiles were taken from this study. The total set of amide I′ profiles of all three protonation states of AAA is shown in Figure 2. The respective profiles look different, but this is due to (a) the overlap with bands outside of the amide I region (CO stretch above 1700 cm^{-1} and COO^- antisymmetric stretch below 1600 cm^{-1} in the spectrum of cationic and zwitterionic AAA, respectively) and (b) the electrostatic influence of the protonated N-terminal group on the N-terminal amide I modes. In the absence of the N-terminal proton the amide I shifts down by ca. 40 cm^{-1}. This leads to a much stronger overlap with the amide I band predominantly assignable to the C-terminal peptide group.[70]

Trialanine Conformations Derived from Amide I′ Simulation Are pH-Independent. In this section we show that the conformational distribution of the central amino acid residue of AAA in aqueous solution is practically independent of the protonation state of the terminal groups. To this end we first analyzed the IR, Raman, and VCD profiles of cationic AAA utilizing the four ^3J-coupling constants dependent on φ and the two $^{2(1)}J$ coupling constants dependent on ψ reported by Graf et al. as simulation restraints.[50] The result of our amide I′ simulation is depicted by the solid lines in Figure 2 and the calculated J-coupling constants in Table 2. The simulation of all amide I′ profiles is in very good agreement with experiment. Table 1 lists the mole fractions, φ and ψ coordinates and half−halfwidths of the resulting subdistributions. A Ramachadran plot of the obtained distribution functions is shown in Figure 3. In agreement with the results of Graf et al.[50] and Schweitzer-Stenner[73]

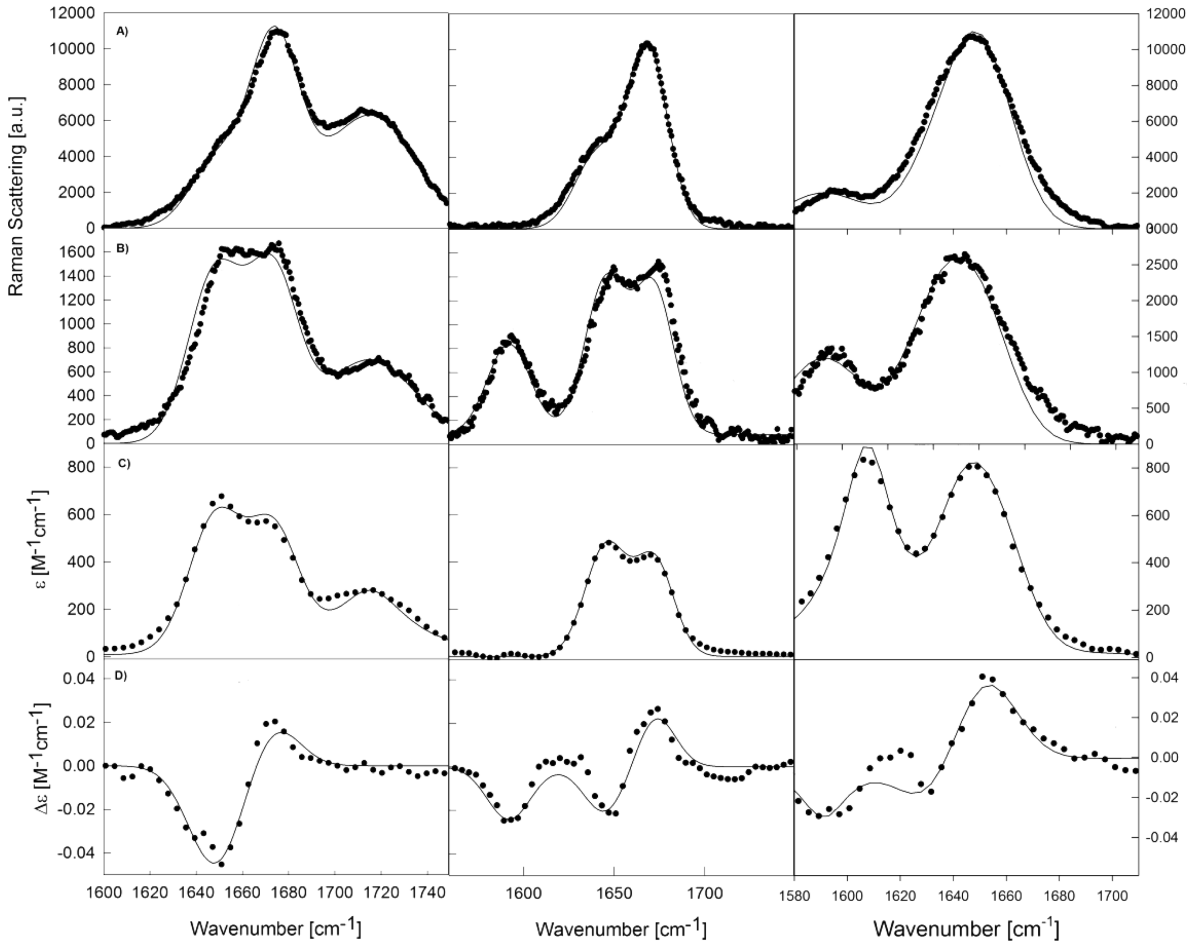

Figure 2. (A) Isotropic Raman, (B) anisotropic Raman, (C) IR, and (D) VCD, band profiles of the amide I′ mode of cationic AAA (left column), zwitterionic (middle column) and anionic (right column) in D_2O. The Raman profiles were taken from Eker et al.[48] The solid lines result from the simulation described in the text.

dx.doi.org/10.1021/jp310466b | J. Phys. Chem. B 2013, 117, 3689−3706

Table 1. Center (φ,ψ)-Coordinates and Respective Mole Fractions of the Two-dimensional Gaussian Sub-distributions Used for Simulation of Vibrational Spectra and J-Coupling Constants for Cationic AAA (AAA+), Zwitterionic AAA (AAA+−), Anionic AAA(AAA−), Alanine Dipeptide (AdP), and Cationic GAG (GAG+)

conformation	AAA+	AAA+−	AAA−	AdP	GAG+
pPII	0.84 (−69,145)	0.84 (−69,145)	0.84 (−69,130)	0.74 (−69,160)	0.72 (−69,155)
β-strand	0.08 (−125,160)	0.08 (−125,160)	0.08(−125,150)	0.16(−115,160)	0.18 (−115,155)
right-hand helical	0.04 (−60,−30)	0.04 (−60,−30)	0.04 (−60,−30)	0.04 (−60,−30)	0.03 (−60,−30)
inverse γ-turn	0.04 (−85,78)	0.04 (−85,78)	0.04 (−85,78)		
type II β-turn				0.03(−60,120)	0.03(−60,−120)
type I′ β-turn				0.03 (20,40)	
inverse γ-turn					0.04(20,−60)

Table 2. Comparison of Experimental[50] and Calculated J-Coupling Constants in Hertz for Cationic AAA

coupling constant	experimental	calculated
$^3J(H^NH^\alpha)$	5.68	5.63
$^3J(H^NC')$	1.13	1.09
$^3J(H^\alpha C')$	1.84	1.57
$^3J(C'C')$	0.25	0.59
$^3J(H^NC^\beta)$	2.39	2.10
$^1J(NC^\alpha)$	11.34	11.19

the analysis reveals a dominant pPII fraction of 0.84, the remaining conformations are β-strand, type II β-turn, right-handed helix and γ-turn-like. These minor fractions were added in order to fine-tune J-coupling constants without deteriorating the simulation of amide I′ profiles. The respective mole fractions of these subconformations certainly carry an uncertainty of up to 5%. It should be mentioned that the fit of the VCD signal required that we assumed an intrinsic magnetic transition moment of 1.1×10^{-23} esu cm. The statistical significance of such weakly populated conformations has recently been discussed in another publication from our group.[79]

Next, we used the obtained conformational distribution function of cationic AAA to simulate the amide I′ profiles of zwitterionic and anionic AAA (Figure1). For the former, we used the $^3J(H^NH^\alpha)$ of the N-terminal amide proton to constrain our simulation. For anionic AAA, we had to use different intrinsic wavenumbers for the individual local amide I modes, since the deprotonation of the N-terminal is known to shift the respective amide I′ mode wavenumber from 1672 to 1635 cm^{-1}.[70] This causes a much larger overlap with the amide I′ band of the C-terminal peptide group (1649 cm^{-1}). Otherwise, we achieved the best fit of the amide I′ band profile of both protonation states with only minor variations of the distribution function obtained for the cationic state. Any significant changes made to either the occupation or breadth of subdistributions defining the conformational ensemble result in less accurate simulations of amide I′ profiles and J coupling constants for both protonation states. The parameters of the conformational distributions for zwitterionic AAA and anionic AAA are listed in Table 1. The $^3J(H^NH^\alpha)$ = 5.74 Hz coupling constant observed for the zwitterionic state was exactly reproduced (Table 3). The

Table 3. Comparison of Experimental and Calculated $^3J(H^NH^\alpha)$ Coupling Constants of Zwitterionic AAA and the Alanine Dipeptide[a]

$^3J(H^NH^\alpha)$	zwitterionic AAA	alanine dipeptide
experimental [Hz]	5.74	5.87
simulation [Hz]	5.74	5.88

[a]All values are expressed in units of Hertz.

respective distribution functions are all plotted in Figure 3. The mole fractions obtained for each conformation remain essentially unaltered among the three different protonation states of AAA. The corresponding subdistributions for all three protonation states of AAA show only slightly different φ and ψ values. Upon deprotonation of the carboxyl group of cationic AAA there is no discernible conformational difference. The most remarkable change is that the pPII distribution shifts to lower ψ-coordinates upon deprotonation of the N-terminal in forming anionic AAA (Table 1). The small difference between the $^3J(H^NH^\alpha)$ coupling constants of cationic ($^3J(H^NH^\alpha)$ = 5.68 Hz) and zwitterionic AAA ($^3J(H^NH^\alpha)$ = 5.74 Hz) are accounted for by a very small shift of the φ-coordinate of the pPII subdistribution. Taken together, our data show *no substantial decrease of the pPII population upon the deprotonation of either termini*, in contrast to what He et al. reported for GxG peptides.[27] Our results also show that differences between $^3J(H^NH^\alpha)$ coupling constants can well reflect small

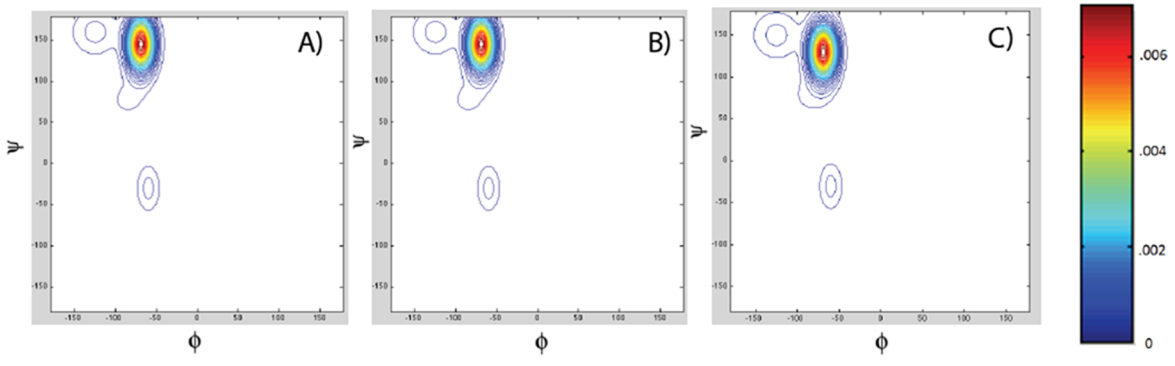

Figure 3. Contour plots depicting the conformational distribution of the central residues of (A) cationic AAA, (B) zwitterionic AAA, and (C) anionic AAA, as obtained from a combined analysis of the amide I′ band profiles in Figure 2, the J-coupling constants reported by Graf et al.[50] for the cationic state, and the $^3J(H^NH^\alpha)$ constant for the zwitterionic state.

dx.doi.org/10.1021/jp310466b | J. Phys. Chem. B 2013, 117, 3689−3706

changes of coordinates of subdistribution rather than variations of their statistical weight. This issue is often overlooked in studies determining conformation in peptides and proteins.[3,13,27,35,44,45,80] Since local residue conformations may significantly differ from canonical values,[10,11,26] assuming static distributions with variant mole fractions may be an oversimplification. Fortunately, our combined analysis of amide I profiles and J-coupling constants, and particularly the sensitivity of the VCD signal strength, is useful for discriminating between population and coordinate changes.[10]

Amide I′ Broadening Is Due Primarily to Correlated Fluctuations of Local Oscillators. While the wavenumber difference of the two amide I′ bands of cationic and zwitterionic AAA are larger than their apparent halfwidths,[5,76] the deprotonation of the N-terminal ammonium group decreases the band splitting and thus increases the overlap between the two bands in the spectrum of the anionic state.[76] In principle, this would affect the validity of the theoretical approach used for the band shape analysis. In this and all earlier studies we used Gaussian profiles to describe the bands associated with individual excitonic transitions.[49] For short peptides like AAA the total bandwidth can be obtained from a self-consistent spectral decomposition of the entire amide I′ band profiles of the Raman and IR-spectra. This yields Voigtian profiles with a Lorentzian bandwidth of 11 cm^{-1} and Gaussian bandwidth between 18 and 23 cm^{-1}.[76] Since the latter is substantially larger than the former, we solely used Gaussian band profiles for our simulations for the sake of computational efficiency. This is a heuristic approach implicitly based on the assumption that all heterogeneities of local amide I oscillators, which are mostly caused by fluctuations due to transitions among different hydrogen bonding configurations,[46,47] are correlated. In other words, we assume that a transition between different arrangements of the peptide-water system causes identical or nearly identical wavenumber changes for both amide I oscillators. As a result, Gaussian distributions of oscillator eigenenergies give rise to Gaussian distributions of excitonic energies. However, if the fluctuations that cause the inhomogeneity of the local oscillators are uncorrelated, the quantum mechanical mixing of interacting vibrational states, which is in first order indirectly proportional to the square of the energy difference between these states, is itself distributed over a certain range of values.[47] For the heavily overlapping amide I bands of, for example, anionic AAA a crossing between energy levels can occur, which can lead to a nearly 50:50 mixing of interacting eigenstates. The situation can become even more complicated if, as suggested by MD simulations, some of the fluctuations are faster than the lifetime of the excited vibrational states.[47,81] This would actually lead to a narrowing of band profiles. In order to check how uncorrelated broadening affects the amide I′ profiles of anionic AAA, we modified our algorithm by inserting Gaussian distributions of local wavenumbers for both amide I oscillators. If Ω_1 and Ω_2 are the eigenenergies of local oscillators that coincide with the peak position of their respective absorption and Raman bands, uncorrelated inhomogeneous broadening of both oscillators can be accounted for by the following distribution function

$$S(\tilde{\nu}) = \frac{\sum_{i=1}^{m_1}\sum_{k=1}^{m_2}\left[\exp\left(-\frac{(\Delta\Omega_{1,i})^2}{2\sigma_1^2}-\frac{(\Delta\Omega_{2,k})^2}{2\sigma_2^2}\right)\left(\frac{S_i\Gamma_1/\pi}{((\tilde{\nu}-(\Omega_1+\Delta\Omega_{1,i}))^2+\Gamma_1^2)}+\frac{S_k\Gamma_2/\pi}{((\tilde{\nu}-(\Omega_2+\Delta\Omega_{2,k}))^2+\Gamma_2^2)}\right)\right]}{\sum_{i=1}^{m_1}\sum_{k=1}^{m_2}\exp\left(-\frac{(\Delta\Omega_{1,i})}{2\sigma_1^2}-\frac{(\Delta\Omega_{2,k})}{2\sigma_2^2}\right)} \quad (13)$$

where $S(\tilde{\nu})$ represents IR, Raman, and VCD intensities, $\tilde{\nu}$ labels the wavenumber position in the spectra, S_i and S_k are intensity parameters that depend on the degree of excitonic coupling associated with the respective differences $\Delta\Omega_{1,i}\Delta\Omega_{2,k}$ between the peak wavenumbers of the individual amide I′ bands and the corresponding wavenumbers representing modes of the inhomogeneous ensemble for which excitonic coupling was calculated. Γ_1, Γ_2 are the half−halfwidth of the Lorentzian profiles associated with the first and the second amide I transition. All contributions with wavenumbers detuned by $\Omega_{1,i}$ and $\Omega_{2,k}$ from the respective peak position are weighted with Gaussian functions with the respective half−halfwidths denoted as σ_1 and σ_2. The numerator describes the convolution of two Voigtian profiles, for which the integrals are substituted by summations. The denominator contains the partition sum of the inhomogeneous ensemble under consideration.

For a first simulation we assumed that the entire inhomogeneous broadening of both amide I modes stems from uncorrelated fluctuations, which are slower than the time scale of absorption (IR, VCD) and scattering (Raman) processes.[47,81] In this case, the Lorentzians in eq 1 should have a half−halfwidth of ca. 5.5 cm^{-1}, which reflects the lifetime of the excited vibrational state.[5] For σ_1 and σ_2 we chose 12 cm^{-1}. We digitized the individual Gaussian profiles with 15 data point between $\Omega \pm 2\sigma$ which resulted in 225 microstates. We used the conformational distribution function derived for anionic AAA to simulate the corresponding amide I′ profile and obtained the results depicted by the solid line in Figure 4. Apparently, the strong mixing between adjacent states of the considered inhomogeneous distribution leads to a rather asymmetric distribution of intensities in the IR as well as in the Raman spectra, which is absent in experimental spectra.[47] Any attempts to close the gap between experiment and simulation by changing the distribution function failed. Increasing the fraction of right-handed helical- (or type III β-turn-) like conformation at the expense of pPII returns the VCD signal to the correct order of magnitude but does not eliminate the asymmetry of the other band profiles.

Next, we tested a less radical solution. We assumed that only part of the inhomogeneous broadening is correlated and replaced the Lorentzian by a Gaussian function in eq 4

$$S(\tilde{\nu}) = \frac{\sum_{i=1}^{m_1}\sum_{k=1}^{m_2}\left[\exp\left(-\frac{(\Delta\Omega_{1,i})^2}{2\sigma_1^2}-\frac{(\Delta\Omega_{2,k})^2}{2\sigma_2^2}\right)\left(\frac{S_i}{\tilde{\sigma}_1\sqrt{2\pi}}e^{-(\tilde{\nu}-(\Omega_1+\Delta\Omega_{1,i}))^2/2\tilde{\sigma}_1}+\frac{S_k}{\tilde{\sigma}_1\sqrt{\pi}}e^{-(\tilde{\nu}-(\Omega_2+\Delta\Omega_{2,k}))^2/2\tilde{\sigma}_2}\right)\right]}{\sum_{i=1}^{m_1}\sum_{k=1}^{m_2}\exp\left(-\frac{(\Delta\Omega_{1,i})}{2\sigma_1^2}-\frac{(\Delta\Omega_{2,k})}{2\sigma_2^2}\right)} \quad (14)$$

dx.doi.org/10.1021/jp310466b | J. Phys. Chem. B 2013, 117, 3689−3706

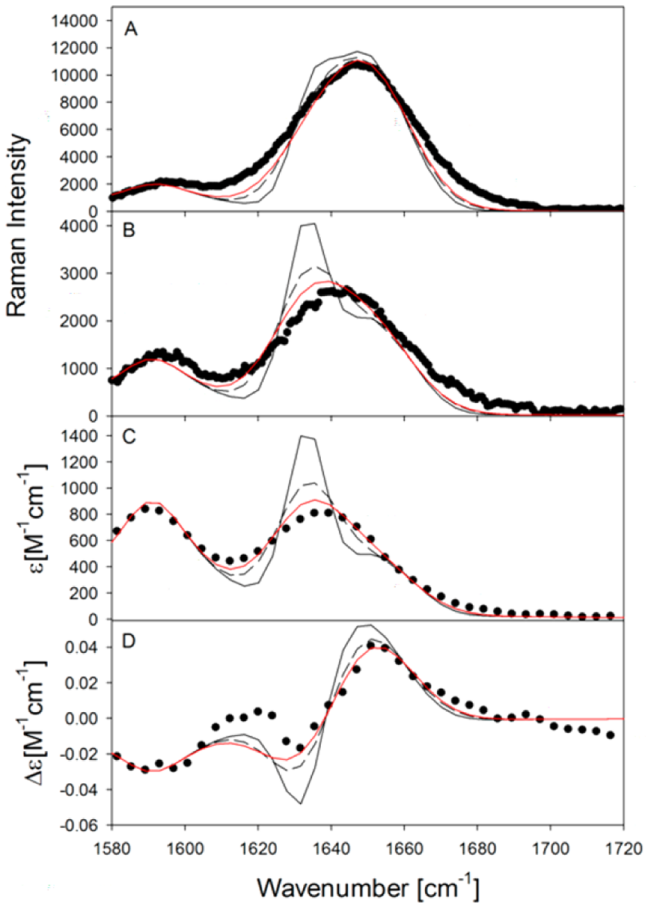

Figure 4. Simulation of the (A) isotropic Raman, (B) anisotropic Raman, (C) IR, and (B) VCD amide I′ band profile of anionic AAA in D_2O with a model which explicitly considers uncorrelated inhomogeneous broadening of the two interaction oscillators. The solid lines result from a simulation for which the natural band profile of the two oscillators (half–half width of 5.5 cm^{-1}) was convoluted with two Gaussian distributions of eigenenergies with a common half–halfwidth of 12 cm^{-1}. For the other two simulations we assumed that part of the inhomogeneous broadening is correlated. The uncorrelated broadening was set to $\sigma_{c,1} = \sigma_{c,2} = 9$ cm^{-1} (dashed) and $\sigma_{c,1} = \sigma_{c,2} = 6.6$ cm^{-1} (red), the respective correlated broadening for the excitonic transitions was $\sigma_1 = \sigma_2 = 8$ cm^{-1} (dashed) and $\sigma_1 = \sigma_2 = 10$ cm^{-1} (red).

where $\tilde{\sigma}_1,\tilde{\sigma}_2$ is the Gaussian half–halfwidth of the correlated inhomogeneous distributions of the two amide I′ band. We carried out several simulation with pairs of $\sigma_{c,i}$ and $\tilde{\sigma}_1 = \tilde{\sigma}_2$. For all cases, we assumed that $((\sigma_{C,i})^2 + (\sigma_i)^2)^{1/2} = ((\sigma_{C,k})^2 + (\sigma_i)^2)^{1/2} = 12$ cm^{-1}. The dashed and red band profiles were calculated with the values $\sigma_{c,1} = \sigma_{c,2} = 9$ cm^{-1}, $\sigma_1 = \sigma_2 = 8$ cm^{-1} (dashed) and $\sigma_{c,1} = \sigma_{c,2} = 6.6$ cm^{-1}, $\sigma_1 = \sigma_2 = 10$ cm^{-1} (red). Only the spectra derived with the latter pair of halfwidth values are sufficiently close to the experimental data to consider the simulation acceptable. However, the simulation with the simple correlated distribution model is still superior. We therefore conclude that the inhomogeneous broadening of the amide I transitions results predominantly from coherent fluctuations of the two amide I oscillators. Hence, we can rely on the simpler model thus far used to analyze amide I′ band profiles. This is a somewhat surprising, since results from MD simulations suggests that both oscillators are affected by uncorrelated motions.[47] However, the amide I IR profiles calculated by explicitly considering these uncorrelated fluctuations derived from DFT and semiclassical line shape theory display rather well resolved individual amide I bands for cationic AAA, which are not observed in experimental profiles.[38,47,81]

Blocked Dipeptides Form Conformational Ensembles Similar to Corresponding GxG Peptides. In this paragraph we add another piece of evidence to support the notion that the termini of tripeptides do not exert a detectable influence on their central residue. We analyzed the amide I′ band profiles of AdP shown in Figure 5. The respective $^3J(H^NH^\alpha)$ constant is

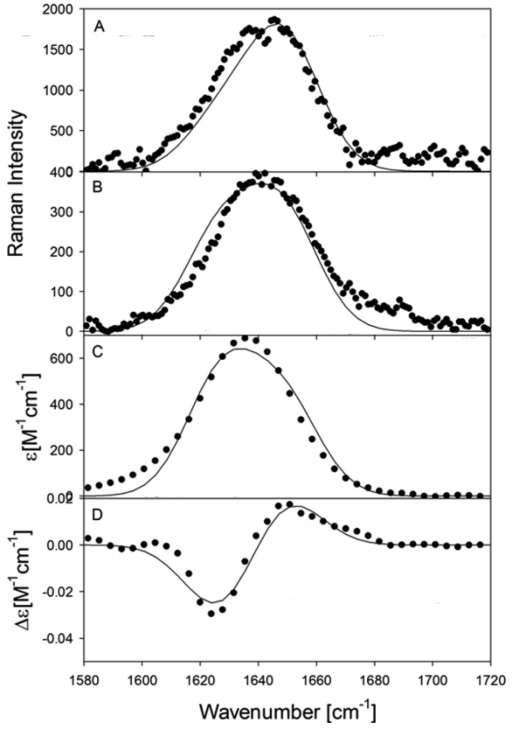

Figure 5. (A) Isotropic Raman, (B) anisotropic Raman, (C) IR, and (D) VCD band profiles of the amide I′ mode of AdP in D_2O. The solid lines result from the simulation described in the text.

listed in Table 3. The IR and Raman profiles are very reminiscent of what we observed for anionic AAA, owing to the absence of the charge on the N-terminal group, but the VCD is negatively biased indicating an intrinsic magnetic moment of the C-terminal.[82] The simulation of the Raman profiles required that we allowed the anisotropy of the Raman tensors of the unperturbed, local modes to be slightly different. The VCD signal was fully reproduced by our simulation as was the $^3J(H^NH^\alpha)$ constant. The resulting substates and their respective statistical weights are listed in Table 1. The pPII fraction of the central alanine residue in the dipeptide is slightly lower than the value observed for all protonation states of AAA. The location of the pPII trough is also downshifted in comparison to trialanine. (Figure S1, Supporting Information). Interestingly, the final distribution for AdP (Table 1) is actually very similar to what Hagarman et al. previously reported for the unblocked GAG peptide.[10] For the sake of comparison, the amide I′ band profiles of GAG are shown in Figure S2 in the Supporting Information. It should be noted that resimulation of these profiles for GAG became necessary because of a minor error in the equation used to fit the $^3J(H^NC')$-coupling constant.[10,50] However, this refitting with the updated equation leads to only very minor adjustments to the conformational

dx.doi.org/10.1021/jp310466b | J. Phys. Chem. B 2013, 117, 3689–3706

distribution of GAG (Table 1). Altogether, the distributions of AdP and GAG (Table 1) agree quite well. Actually, this is what one might expect in view of the fact that in both GAG and AdP peptides, the two peptide bonds surrounding the central alanine residue are directly flanked by methylene and methyl groups respectively (i.e., the blocked terminal CH_3-groups of AdP are more reminiscent of glycine than of alanine residues since glycine lacks a β-carbon.) This conformational similarity shows that the interaction between dipeptide termini with the central residue is analogous to the (most likely weak) interaction between terminal glycines and the central residue in GxG, meaning that the strength of nearest neighbor interactions is practically absent for any atoms beyond neighboring Cα side-chains. The only remaining difference between GAG and AdP are the free termini of glycine which are absent in AdP. Since we find that the central alanine residue in these two peptides have nearly identical conformational ensembles our results demonstrate a very limited influence of terminal charges on nonionized central residues of tripeptides.

To check the generality of the above results for nonalanine residues, we examined the unblocked fully protonated Gly-Val-Gly (GVG) peptide and the valine dipeptide (VdP). Figure S3 and S4 (Supporting Information) show the polarized Raman, IR, and VCD, amide I′ profiles and simulation for GVG[10] and VdP. The negative couplet in the VCD spectra for GVG is obviously weaker than that of GAG, indicating a decreased sampling of the pPII conformation for valine residues. Following the same theoretical protocol as described above (see Sec. Theory), we simulated all amide I′ profiles for GVG utilizing the six conformationally sensitive J-coupling constants as restraints.[10] The final fit to experimental data is plotted as the solid lines in Figure S2 and S3 (Supporting Information). The $^3J(H^NH^\alpha)$ coupling constants for both valine peptides are very well reproduced by our simulation procedure (Table S3, Supporting Information). The thus obtained conformational distributions for GVG and VdP (Table S1, Supporting Information) are both similar to those recently reported for the GVG peptide.[10,83] In contrast to the alanine peptides, GVG has a decreased pPII content (χ_{pPII} = 0.32) in preference for an increased sampling of β-strand-like conformation (χ_β =0.46). The φ and ψ coordinates of these subdistributions are also shifted to lower and higher values, respectively, as compared to those obtained for the alanine-based peptides. Similar to the case of alanine peptides, the experimental data for the VdP could be reproduced with nearly the same conformational distribution and statistical weights obtained for GVG. This result demonstrates once again that there is limited conformational influence of terminal groups on central residues in tripeptides, and moreover, that the similarity of uncapped glycine termini to methyl-blocked termini holds true for peptides with non pPII-preferring central residues. While these results indeed show negligible end-group effects on conformations of aliphatic residues in tripeptides, one might still expect a different situation for polar and/or ioniziable side chains. However, recent studies by Rybka et al. have shown that even aspartic acid, which has an unusually high asx turn-propensity, samples the same conformational manifold in a free glycine environment (GDG) and in the blocked dipeptide (DdP).[83] Taken together these results indicate that *the conformational ensemble sampled by GxG peptides closely mimics those of the corresponding dipeptides*, again suggesting negligible influence of the termini protonation state on intrinsic propensity.

The Gibbs Energy Landscape of Alanine Residues in Unblocked Tri- and Blocked Dipeptides Is Not Influenced by End-effects. To further explore the factors stabilizing the conformational distributions of the three alanine based peptides (cationic AAA, zwitterionic AAA, and AdP), we characterized their ensembles in thermodynamic terms. While the above studies revealed very limited differences between the protonation states of AAA and AdP, it is possible that differences emerge at, for example, higher temperatures because of different enthalpic and entropic contributions between coexisting conformations. Indeed, an analysis of CD spectra of cationic and zwitterionic AAA has led Oh et al. to the conclusion that the thermodynamic parameters of the two protonation states are different.[80] In a first step, we measured the far UV-CD spectra of zwitterionic AAA and Adp as a function of temperature between 5 and 85 °C, which are shown in Figure 6. Previously recorded UV-CD spectra of cationic AAA measured between 0 and 90 °C[61] are also shown in Figure 6 for comparison. To facilitate the comparison of the investigated peptides, they are all plotted on the same scale in units of $\Delta\varepsilon$ [M^{-1} cm^{-1} $residues^{-1}$], where the number of residues contributing to the CD signal for AAA and AdP are 2 and 1, respectively. At low temperature, all three of these alanine based peptides exhibit CD signals characteristic of a dominant sampling of pPII conformation, in agreement with

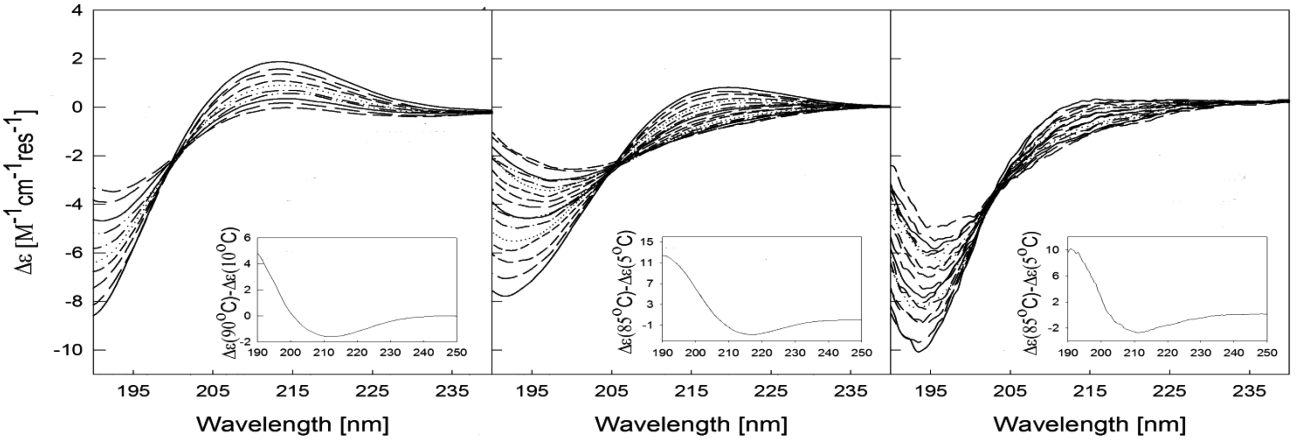

Figure 6. UVCD spectra of (A) cationic AAA, (B) zwitterionic AAA, and (C) the AdP as a function of temperature. Cationic AAA spectra range from 0 to 90 °C with ΔT = 10 °C. Zwitterionic AAA and the alanine dipeptide range from 5 to 85 °C with ΔT = 5 °C.

dx.doi.org/10.1021/jp310466b | J. Phys. Chem. B 2013, 117, 3689−3706

literature.[1,84,85] Cationic AAA is most prominent in this regard, with a positive maximum at approximately 215 nm and a pronounced negative maximum at 190 nm. The insets in Figure 6 depict the difference spectra calculated by subtracting the lowest temperature spectra from the highest temperature spectra. They are all indicative of a population redistribution from pPII to more β-like conformations.[50,61,84,86,87]

A word of caution deserves to be mentioned here regarding the use of CD to characterize peptide conformation. Although CD spectra can provide powerful qualitative information, the sole use of this technique to define conformational populations in peptides is problematic and may not yield unambiguous results. However, the ability of CD to track spectral *changes* reflecting population redistributions with e.g. changing temperature can indeed provide useful information regarding the energetics of the system, especially when backed up by *a priori* knowledge of conformational subspace.

Although the temperature dependence of the CD spectra for all three alanine based peptides is qualitatively similar, a direct comparison of cationic AAA zwitterionic AAA and AdP reveals distinct differences in the spectral line shape at all temperatures. As reported earlier,[27,80] the spectra for zwitterionic AAA is noticeably red-shifted as well as lower in intensity at both the positive and negative maxima compared to that of cationic AAA. It is not likely that this difference is due to structural changes as this would be reflected in a significant change in the $^3J(H^NH^\alpha)$ constants for each peptide, contrary to our experimental results. More likely, this pH-dependent spectral change is due to interference of the charge transfer (CT) band between the C-terminal carboxylate and the peptide group of zwitterionic AAA. This band has been previously reported by Pajcini et al.[88] for glycylglycine and by Dragomir et al for AX and XA peptides, and is assignable to a $n_{coo}\rightarrow\pi^*$ transition.[89] Dragomir et al. showed that the frequency position of this CT band correlates well with the positive dichroic maxima of pPII in the respective CD spectrum.

A comparison of the CD spectra of cationic AAA with AdP reveals differences in line shape at both low and high temperatures. Because AdP is blocked at the C-terminal carboxylate, these spectral changes cannot be a result of the CT transition. The positive maximum at 210 nm, diagnostic of pPII conformation, is noticeably decreased for AdP relative to cationic AAA, indicating less sampling of pPII-like conformation in favor of more extended conformations. This is in agreement with the results from our present vibrational analysis where we obtain a slightly lower pPII fraction for AdP and an increased β-content relative to both cationic and zwitterionic AAA.

The temperature dependence of the CD for each peptide displays an isodichroic point (Figure 6), indicating that all three peptides predominantly sample two conformational states within the temperature region (i.e pPII- and β-like). This two-state behavior is typical of short alanine-based peptides,[77,78,90] and is again in line with the conformational ensembles obtained for these peptides through the simulation of the amide I′ vibrational profiles (Table 1).

In order to investigate the free energy landscape of each alanine peptide, we employed a global fitting procedure to analyze the temperature dependence of the conformationally sensitive maximum dichroism $\Delta\varepsilon$ (T) and the $^3J(H^NH^\alpha)(T)$ values with a two-state pPII-β model (see Sec. Theory).[25,61] To be consistent with the conformational ensembles of each peptide derived above, we began the fitting process by using the statistical average $\langle^3J_{pPII}\rangle$ and $\langle^3J_\beta\rangle$ of, and the Gibbs energy difference between, the pPII and β distributions derived from our vibrational analysis (see sec. Theory). However, this process originally led to a poor fit to the experimental $^3J(H^NH^\alpha)(T)$ data. This is likely due to the presence of more than two substates in the conformational ensembles of the investigated peptides. For both ionization states of AAA, vibrational analysis revealed that 8% of the conformational ensemble is not of pPII/β type. For AdP this number is 11% (Table 1). To compensate for this slight deviation from two-state behavior we lowered the average φ_{pPII}-value, representing the center of the pPII subdistribution, relative to that obtained from our vibrational analysis. Thus, we decreased $\langle^3J_{pPII}\rangle$. The best fit to the thermodynamic data was achieved by lowering φ_{pPII} by 0.25° and 0.36° per 1% population of non-pPII/β conformations for AAA and AdP, respectively. The thus modified distribution was subsequently used to calculate statistical average $\langle^3J_{pPII}\rangle$ and $\langle^3J_\beta\rangle$ expectation values via the newest version of the Karplus equation.[50] The final values of $\langle^3J_{pPII}\rangle$ and $\langle^3J_\beta\rangle$ obtained from this procedure are 5.02 and 9.18 Hz, respectively, for cationic AAA, 5.09 Hz and 9.18 Hz for zwitterionic AAA, and 4.69 Hz and 9.17 Hz for AdP (Table 4). We used these 'effective' reference coupling constants and the respective experimental $^3J(H^NH^\alpha)$ values to calculate the mole fractions of pPII and β-strand conformations for the residues in each alanine peptide. This procedure results in pPII mole fractions for the central residues, $\chi_{i=1}$(pPII), of 0.86, 0.84, and 0.74 for cationic AAA, zwitterionic AAA, and AdP, respectively (Table 4), which exactly match the mole fractions we derived from our vibrational analysis of amide I′ modes (Table 1). This shows that our forced reduction to a two-state model for the thermodynamic analysis indeed preserved the Gibbs energy difference between the pPII and β-strand conformations. This observation indicates that the population of turn conformations might not be very temperature dependent, in agreement with recent theoretical predictions and experimental results.[83,91] For the C-terminal residue, we obtained pPII fractions of 0.67, 0.60, for cationic and zwitterionic AAA, respectively.

Using the calculated reference $\langle^3J\rangle$ values obtained, we could then employ eq 6 (see sec. Theory) to fit the experimental ^3J(T) data and extract thermodynamic information regarding the pPII/β-strand equilibrium for all peptides. The resulting fits for all three peptides are shown as solid lines in Figure 7. The thermodynamic parameters obtained from this procedure are shown in Table 4. For the central residue of cationic AAA we

Table 4. Spectroscopic and Thermodynamic Parameters Derived from Fitting the Temperature Dependence of the $^3J(H^N,H^\alpha)$ Coupling Constants for Cationic AAA (AAA^+), Zwitterionic AAA (AAA^{+-}), and the Alanine Dipeptide (AdP) using the Two-state Fitting Procedure Described in the Text

	$^3J(H^NH^\alpha)$	J(pPII) [Hz]	$J(\beta)$ [Hz]	χ_1(pPII)	ΔG_1 (kJ/mol)	ΔH_1 (kJ/mol)	ΔS_1 (kJ/mol)	χ_2(pPII)	ΔG_2 (kJ/mol)	ΔH_2 (kJ/mol)	ΔS_2 (kJ/mol)
AAA^+	5.61	5.02	9.18	0.86	−4.44	−20.6	−54.4	0.67	−1.71	−10.63	−29.92
AAA^{+-}	5.74	5.09	9.18	0.84	−4.41	−20.6	−55.32	0.6	−1.01	−10.63	−32.27
AdP	5.87	4.63	9.17	0.74	−2.50	−25.2	−66.1				

dx.doi.org/10.1021/jp310466b | J. Phys. Chem. B 2013, 117, 3689−3706

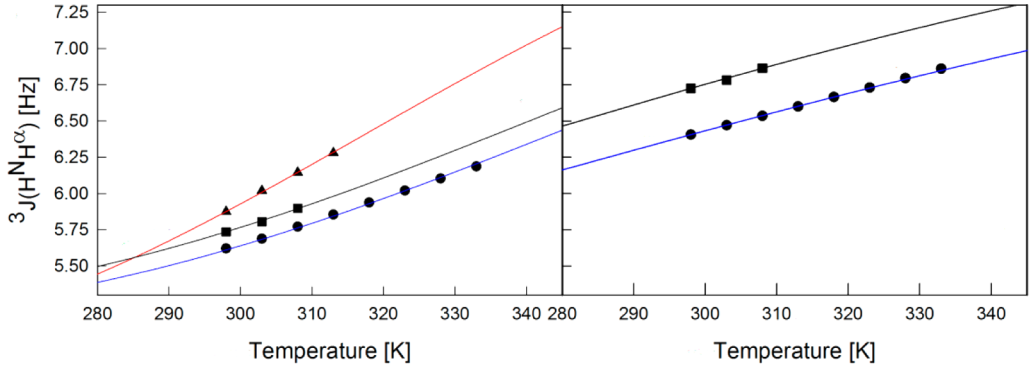

Figure 7. $^3J(H^N,H^\alpha)$ [Hz] of the central (left panel) and C-terminal residue amide (right panel) plotted as a function of temperature for cationic AAA (circles), zwitterionic AAA (squares) and the AdP (triangles). The solid lines result from the two-state thermodynamic model fitting procedure described in the text.

obtain $\Delta G_1 = -4.44$ kJ/mol at room temperature, with an enthalpic difference between pPII and β-strand of $\Delta H_1 = -20.7$ kJ/mol, whereas the entropy difference is $\Delta S_1 = -54.4$ J/mol·K. These values are all somewhat larger than those obtained by Oh et al., who simultaneously analyzed CD and ^{H}NMR data of cationic AAA using an iterative approach to find reference J_{pPII} and J_β values.[80] Their analysis yielded $\Delta H = -10.63$ kJ/mol and $\Delta S = -50.2$J/mol·K. In contrast, our values are only slightly lower than those obtained by the joint MD/NMR studies of Graf et al.[50] ($\Delta H = -24.8$ kJ/mol and $\Delta S = -62.2$ J/mol·K), where each reference coupling constant was calculated by directly averaging the Karplus-derived coupling constants over all MD conformations within the substate. In view of the uncertainties of the obtained thermodynamic parameters our results and those reported by Graf et al. can be considered as being in reasonable agreement. In a previous study on solvation effects on the conformation of AAA,[61] we employed a slightly different fitting approach, using central and C-terminal residue thermodynamic parameters to calculate the temperature dependence of the effective equilibrium constant and Gibbs free energy for the net pPII↔β-strand transition, which was then used to fit the $\Delta\varepsilon$(T) data. However, we have since revised our $\Delta\varepsilon$(T) fitting procedure to explicitly account for the contributions from the four different peptide conformations (see eq 6).[25] The thermodynamic values obtained with the revised equation are qualitatively similar to those listed by Toal et al.,[61] although slightly less negative. For zwitterionic AAA, our analysis yielded Gibbs free energy differences at room temperature for the pPII↔β-strand transition of $\Delta G_1 = -4.17$ kJ/mol and $\Delta G_2 = -1.01$ kJ/mol, which are noticeably similar to those obtained for cationic AAA ($\Delta G_1 = -4.44$ kJ/mol and $\chi_{2,pPII} = 0.67$, $\Delta G_2 = -1.71$ kJ/mol). To further explore whether there is an influence of the terminal groups on the thermodynamics of zwitterionic AAA we used the ΔH_i values obtained from $^3J(H^NH^\alpha)(T)$ of cationic AAA to fit the corresponding data of zwitterionic AAA. The resulting fit is in good agreement with the experimental data (Figure 7), indicating that *the free energy landscape of unblocked AAA is indeed very similar across all protonation states*. From this fit to zwitterionic AAA data we obtain slightly higher entropic contributions for both residues (i.e, $dS_1 = -55.3$ J/mol·K for the central residue and $dS_2 = -32.3$ J/mol·K for the C-terminal) as compared to cationic AAA (Table 4).

To fit the experimental HNMR data for the AdP, we were restricted to a single set of $^3J(H^HH^\alpha)(T)$ data as AdP does not have a second amide proton coupled to a C_α proton. As described above, using the distribution obtained from amide I′ profiles and the experimental room temperature value of $^3J(H^NH^\alpha) = 5.8$ Hz, we obtain a pPII population of $\chi_{1,pPII} = 0.74$, in agreement with our vibrational analysis. This population is associated with a Gibbs free energy difference between pPII and β-strand of $\Delta G_1 = -2.5$ kJ/mol (Table 4). The result of the final fit using dH_i as the sole free parameter is shown in Figure 7. From this fit, the corresponding ΔH_1 and ΔS_1 values were obtained (i.e., $\Delta H_1 = -22.2$ kJ/mol and $\Delta S_2 = -66.1$J/mol·K), which are slightly larger than the respective values obtained for both protonation states of AAA (Table 4).

With the thermodynamic parameters for each peptide derived above, the analysis of the $\Delta\varepsilon(T)$ data could be carried out using the Boltzmann distribution factors in eq 6 and eq 7 for AAA and AdP, respectively. The final fit to the experimental data is shown as solid lines in Figure S5 (Supporting Information). From this analysis we obtain the conformation-specific spectroscopic parameters, $\Delta\varepsilon_{pPII}$ and $\Delta\varepsilon_\beta$, which are listed for each peptide in Table S2 (Supporting Information).

MD Reveals that the pPII Content and Hydration Shell of AAA Remains Intact upon Switching Protonation States. To further investigate the ensemble differences of the three alanine-based peptides in atomistic detail we performed a series of all-atom MD simulations combining two of the currently available force fields (OPLS and AMBER03) with the three commonly used water models (TIP3P, SPCE, TIP4P). The AMBER03 force field was also used in combination with with the TIP4Ew water model. Our decision to test multiple force-field/water models combinations stems from the poor reproduction of experimentally obtained distributions for short peptides and unfolded proteins reported in many MD studies. It is now well-known that different force fields yield rather different conformational distributions, typically producing very low pPII propensities and overestimating the helical content, at variance with experimental results.[30,32,36,43,54,92] In addition, the use of different water models for explicit solvation also leads to variable conformational preferences.[93] Here, we chose to gauge, which of the above-mentioned force-field/water model combinations would predict conformational ensembles in the best agreement with experimental data, and then use this combination for a direct comparison of the two different alanine model systems.

In order to obtain conformational propensities, we defined the (φ,ψ) angles corresponding to the peak position for each major conformation (i.e., pPII-, β strand-, and helical-like) by first identifying the centers of each distribution in the MD-derived Ramachadran plots. The spread of each subpopulation was then defined by ensuring that all respective conformations were included, similar to the method employed by to

dx.doi.org/10.1021/jp310466b | J. Phys. Chem. B 2013, 117, 3689−3706

Table 5. Fraction of pPII, β-Strand and Helical-like Conformations Obtained from MD Simulations of Cationic AAA, Zwitterionic AAA, and AdP using the OPLS, Amber 03, and Amber 10 Force Fields with the TIP3P, TIP4P, and SPC/E Explicit Water Models

		cationic AAA				Zwitterionic AAA				alanine dipeptide			
force field	conformation type	TIP3P	SPC/E	TIP4P	Tip4p-Ew	TIP3P	SPC/E	TIP4P	Tip4p-Ew	TIP3P	SPC/E	TIP4P	TIP4p-Ew
OPLS	pPII	0.6	0.67	0.62		0.54	0.53	0.57		0.44	0.47	0.45	
	B-strand	0.12	0.11	0.15		0.13	0.12	0.15		0.12	0.11	0.14	
	Helical-like	0.17	0.13	0.15		0.12	0.13	0.08		0.23	0.22	0.22	
	remainder	0.105	0.09	0.06		0.21	0.22	0.2		0.11	0.2	0.19	
Amber 03	pPII	0.58	0.61	0.59	0.39				0.39	0.37	0.41	0.34	0.39
	B-strand	0.22	0.19	0.24	0.15				0.15	0.16	0.16	0.17	0.15
	Helical-like	0.09	0.08	0.06	0.34				0.34	0.35	0.3	0.36	0.34
	remainder	0.11	0.12	0.11	0.12				0.12	0.12	0.13	0.13	0.12

Gnanakaran and Garcia.[21] Table 5 shows the resulting fractions of pPII, β-strand, and helical-like conformations sampled during all MD simulations. By comparing the results for different force-field/water model combinations, we noted that the OPLS force-field yielded the most accurate reproduction of the experimentally obtained conformational distributions and conformer statistical weights for cationic AAA. Not surprisingly, the fractions of pPII obtained with the OPLS force-field are still below what we and others obtain experimentally,[1,50,73] but the discrepancy between experiment and theory is relatively modest compared with what resulted from earlier MD simulations performed with force fields which were not drastically modified.[43,53,54,57,58,93,94] pPII fractions emerging from these studies do not normally exceed 0.5. The helical content obtained from our simulations is still above what is expected for short peptides. This overestimation of the right-handed helical content is characteristic of most MD simulations involving unfolded proteins or short peptides.[30,32,43,54,92,93,95] Although our MD results are not yet in full quantitative agreement with experiment, they are sufficient for our purposes of investigating the relative population differences between the three alanine peptides.

Of all the water models under study, the SPCE water model yielded the best agreement with experiment, that is, the greatest sampling of pPII conformations for cationic AAA and AdP. Figure 8 shows the corresponding Ramachandran plots for cationic AAA, zwitterionic AAA, and AdP obtained using the OPLS force field with the SPC/E water model. All three plots clearly show a dominant sampling of the pPII conformations followed by β-strand-like (i.e., extended) conformations. They suggest further that both protonation states of AAA have a relatively higher pPII fraction compared to AdP, again in agreement with our vibrational and thermodynamic results. It should be noted that MD simulations yielded a slightly higher pPII content for the cationic compared with the zwitterionic state of AAA. However, no increase in the β-strand or helical conformations was observed in the latter. Instead, the Ramachandran plot in Figure 8 indicates a scattered population close to the bridge region between the β-strand and the right-handed helical region which with respect to φ are spread in the region located between −140° and −90°. An increased population in this region would certainly cause an increase of the $^3J(H^NH^\alpha)$ in the zwitterionic state with respect to the value observed for the cationic state, which is larger than the very small experimentally obtained change As shown above, this has not been obtained.

To obtain information on the dynamics of the conformational ensemble, the time evolution of the dihedral angles φ and ψ was monitored (Figure S6) throughout the 50 ns MD trajectory for cationic AAA and AdP. To calculate the lifetimes and hence the stability of each conformation, the time

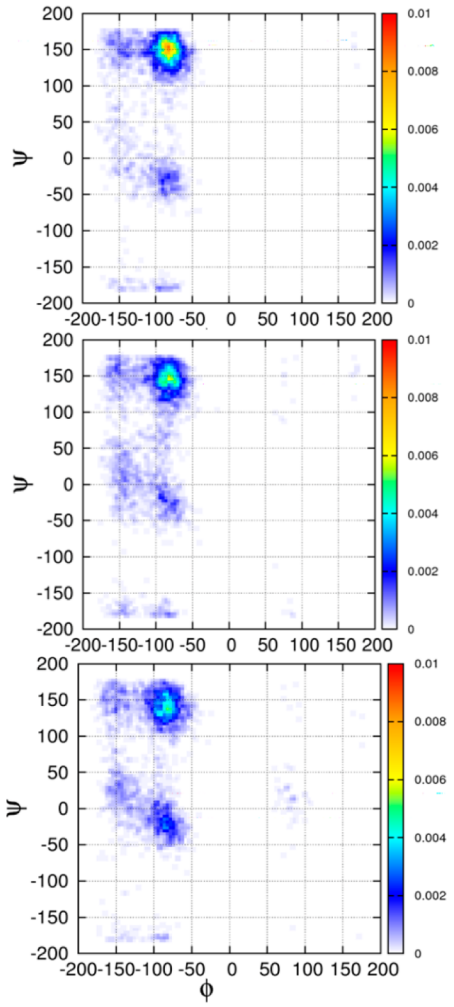

Figure 8. Ramachandran plots for (A) the cationic and (B) zwitterionic AAA and (C) AdP obtained by MD simulations using the OPLS force field and SPC/E water model.

durations of the three conformations along the MD trajectory were extracted Figure 9 shows the distributions of the time durations, N(t), for each of the three major conformations. The lifetime (τ) of each conformation was determined by fitting each curve with an exponential function. Notably, all time distributions shown in Figure 9 could be fit accurately with a single exponential function, except for the pPII distribution of AAA which required a biexponential fit. Table 6 lists the obtained lifetimes for each major conformation sampled by

dx.doi.org/10.1021/jp310466b | J. Phys. Chem. B 2013, 117, 3689−3706

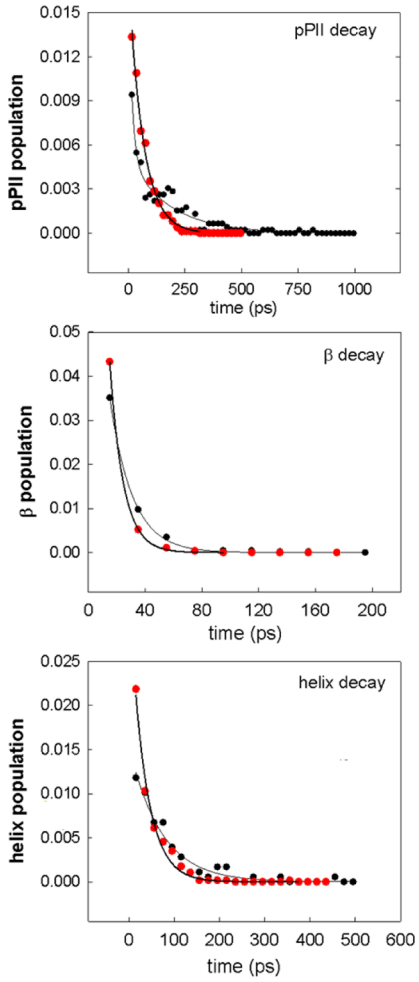

Figure 9. Distribution of durations, $N(t)$, of the (A) pPII, (B) β-strand, and (C) helical conformations for cationic AAA (black circles) and AdP (red circles) derived by MD. The solid line represents exponential fits (see Table 7, Supporting Information).

AAA and AdP. In general, the pPII conformation persisted for the longest lifetime in both alanine-based peptides. For AAA, the biexponential fit yielded two average lifetimes of 15.8 and 181.8 ps. The two lifetimes likely reflect inhomogeneities with respect to the water distribution within the hydration shell. For AdP, we obtained an effective pPII lifetime of 63.7 ps, which lies approximately in-between the two lifetimes obtained for the same process in AAA. The absence of a fast phase in the decay curve of the pPII conformation of AdP might have been due to the 20 ps time resolution of the MD simulations. In both peptides, the helical conformation were found to have the longest lifetime, followed by the β-strand conformations. Not surprisingly, the β/pPII transitions were the most frequent for each peptide, in agreement with the largely two-state character of the obtained conformational ensembles. It is noteworthy that the pPII distribution of duration times, $N_{pPII}(t)$, was dominated by the pPII→ β transition, as evidenced by the comparatively large effective rate constant listed in Table S4 (4.14×10^9 s^{-1} and 3.94×10^9 s^{-1} for Adp and AAA, respectively, Supporting Information). Similarly, the β decay was dominated by the β→ pPII transition (4.0×10^9 s^{-1} and 4.10×10^9 s^{-1}, respectively). Such a fast exchange dynamics in cationic AAA has been obtained earlier by Mu and Stock.[58] For illustration, a detailed account of all transition statistics is given in the Supporting Information (Tables S3–4). However, it must be reemphasized again that this notion applies only to the fast phase of the pPII decay discussed above. Surprisingly, a comparison of the three lifetimes for AAA and AdP (Table 6), shows that all conformer

Table 6. Average Lifetime (τ), and Initial Population (N_0), and R^2 Paramaters Obtained from Fitting Duration Distribution Curves, N(t), for Cationic AAA and AdP in Each Major Conformation[a]

	conformation	N_0	τ (ps)	R^2
Trialanine	pPII	0.0084/0.0051	15.77/181.81	0.976
	β	0.0898	15.95	0.990
	Helix	0.0154	70.4	0.985
Alanine Dipeptide	pPII	0.0175	63.7	0.996
	β	0.2071	9.58	0.999
	Helix	0.0326	34.6	0.993

[a]Each curve was fit with a single-exponential function, except for the pPII curve of AAA which required a bi-exponential fit and 4 parameters.

lifetimes were significantly shorter for AdP. The large disparity between lifetimes of the three major conformations adopted by the two peptides would not necessarily be expected based soley on differences in conformational propensity. For instance, although the helical conformation had the lowest propensity for all peptides, it had a relatively long effective lifetime (70.4 ps and 34.6 ps for AAA and AdP, respectively) as compared to the lifetime of β-strand (15.95 and 9.58 ps, respectively). This disparity of lifetimes between AAA and AdP and this the stability of the three conformations can be explained by considering the role of the solvent in stabilization of pPII, β-strand, and helical conformations.

In order to more closely investigate the solvation of the three alanine peptides, we calculated the radial pair distribution functions g(r) between the amide proton of the central residue and water hydrogen and oxygen for AAA and AdP (Figure 10A). For the sake of clarity, we omit here the corresponding $g(r)$ plots for zwitterionic AAA as these were near identical to cationic trialanine. Most of the water oxygen atoms were at the hydrogen bonding distance (approximately 1.7 Å) for both protonation states of AAA. In addition, there is a rather intense second maxima in the $g(r)$ for the water oxygen observed at approximately 3.2 Å, reflecting some degree of water ordering, resulting in a pronounced second hydration shell around the central amide atom of AAA. Again, we did not observe any significant differences between $g(r)$ curves of protonated and zwitterionic AAA, indicating that the hydration shells remained intact upon switching the protonation state. For AdP the H_2O-HN distance with the highest water density was increased to about 2 Å and is noticeably less pronounced (by a factor of 3), suggesting a relatively limited hydration of, and weaker hydrogen bonding to, the alanine residues in blocked peptides. This indeed would affect the propensity of the central alanine residue, specifically decreasing the pPII preference for AdP, in agreement with our experimental results. In addition, and perhaps more importantly, the second hydration shell present in AAA was not observed in the dipeptide analogue. The decreased density of water around AdP and the absence of the second hydration shell indicate a much less ordered solvent structure in AdP (relative to AAA). This more disordered solvent structure around AdP was also reflected in a broader distribution of the distance between the central Cβ atom and the C-terminal amide nitrogen atom (Figure 10C), which had

dx.doi.org/10.1021/jp310466b | J. Phys. Chem. B 2013, 117, 3689–3706

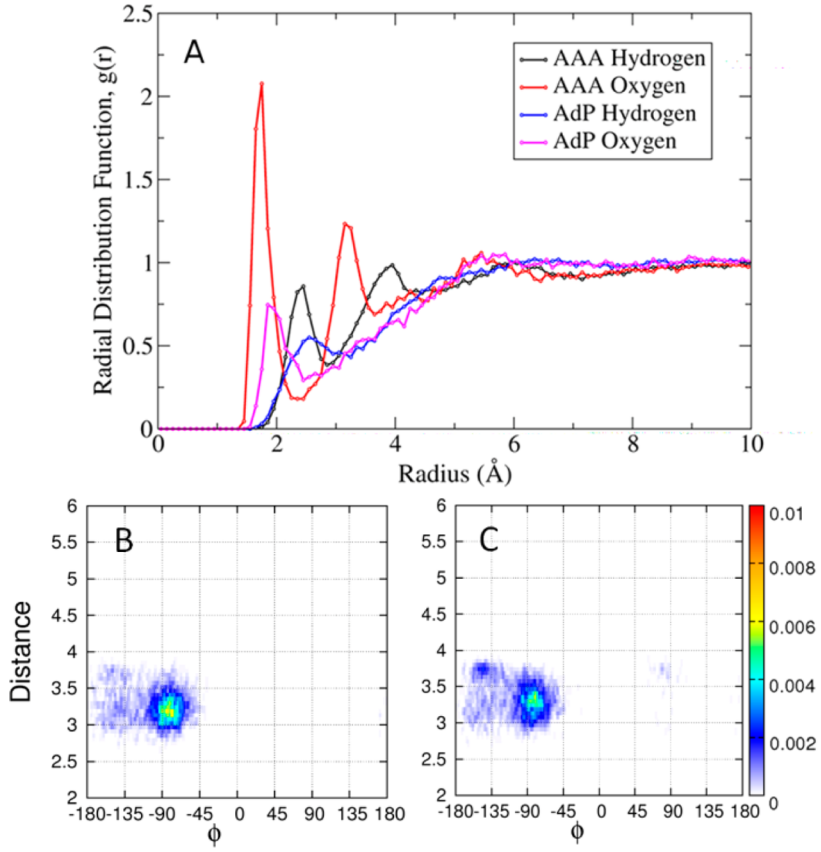

Figure 10. Radial distribution functions, $g(r)$, of water molecules (using H- and O-atoms of water) around the amide proton of the central residue of cationic AAA and AdP (see Figure 1, atoms depicted in blue), derived by MD. Distributions of the (B) cationic AAA and (C) AdP conformations with respect to the dihedral angle φ and the distance between the nitrogen atom of the third residue and the side-chain atom C_β of the central residue in AAA and the corresponding distance in AdP (see Figure 1, the two atoms depicted in red).

additional peaks at larger distances relative to AAA (Figure 10B). The highly ordered solvent structure around AAA and the increased H-bonding capacity can be thought of as effectively increasing the activation barrier between conformations, which indeed explains the aforementioned longer conformational lifetimes obtained for AAA.

Structure Analysis of Blocked Dipeptides in the Literature. The number of papers reporting a structure analysis of the unblocked tripeptides in solution is rather limited; the most relevant of which have been cited in this paper.[5−7,10,24−26,47−49,89] Experimental work on e.g. AAA, the classical model system of unblocked tripeptides, essentially agrees in suggesting a large pPII content of its conformational distribution.[50,73] On the contrary, the body of work on blocked dipeptides, particularly AdP, is voluminous,[29,30,32,36,37,41−43] starting with the computational work of Ramachandran, Flory, and their co-workers who introduced this peptide as a model system for exhibiting random coil behavior.[18,19] This view changed only when Han et al. reported the results of DFT calculations on AdP in explicit water which clearly revealed a preference for pPII.[8] Some experimental studies on AdP and other dipeptides are noteworthy. Kim et al., for instance interpreted the results for two-dimensional IR spectroscopy of AdP in water as indicative of a dominant population of conformation with (φ,ψ) = (−70°, 120°), which they described as pPII, but which resembles more conformations found at the i+1 position of type II β-turns.[96] This study reported a very weak effective coupling constant of 1.5 cm^{-1}, which is somewhat surprising since it is inconsistent with the rather strong VCD signal in Figure 5. Weise et al. measured and analyzed dipolar coupling constants of AdP in the lyotropic liquid-crystalline solvent cesium pentadecafluorooctanoate in water and found evidence for pPII being the most stable conformation of the peptide.[15] In a very comprehensive study, Grdadolnik et al. used the amide III profile of 19 blocked dipeptides in water to identify fractions of pPII, β-strand and right-handed helical conformations.[13] For AdP they found χ_{pPII} = 0.6, χ_β = 0.29 and $\chi_{rhelical}$ = 0.11. This distribution contains slightly more β-strand and helix-like population than the ensemble obtained in the present study suggests (Table 1). The respective fractions reported for VdP are χ_{pPII} = 0.47, χ_β = 0.51 and $\chi_{rhelical}$ = 0.02, which when compared with our distribution (Table 5S, Supporting Information) overestimates both, pPII and β conformations resulting in a nearly isoenergetic free energy landscape. Generally, the differences between the results of our analysis for AdP and VdP and those reported by Grdadolnik et al. are quantitative rather than qualitative. They may be a result from complications in interpreting the amide III region due to its multiplet structure and dependence of its normal mode compositions on vibrational mixing with side chains.[71]

SUMMARY

Taken together, our experimental and MD data show no substantial decrease of the pPII population upon deprotonation of terminal groups, in contrast to what was recently reported in literature.[27] Conformational distributions were obtained from a global analysis of amide I′ bands of IR, polarized Raman, and vibrational circular dichroism spectra and a set of 6 different

dx.doi.org/10.1021/jp310466b | J. Phys. Chem. B 2013, 117, 3689−3706

J-coupling constants. Our combined simulation of these amide I′ profiles and J-coupling constants reveals that the conformational distribution of the central residue in AAA predominantly adopts the pPII conformation (χ_{pPII} = 0.84), followed by the β-strand conformation (χ_β = 0.08), along with small admixtures of right-hand helical-like (χ_α = 0.04) and γ turn-like conformations (χ_γ = 0.04), *in all protonation states*. The proximity of the end groups did not seem to affect this high pPII preference of alanine. Remarkably, the entire conformational distribution, defined by a superposition of Gaussian functions representing the maxima and widths of each substate in (φ, ψ) space remain quantitatively similar in all protonation states of the unblocked tripeptide. In contrast, the pPII fraction of the AdP is slightly lower than what is observed for AAA. Thermodynamic analysis of the alanine-based peptides reveals that the free energy landscape of the pPII-β equilibrium as well as the enthalpic stabilization of the pPII conformation is invariant to terminal charge. Interestingly, the conformational ensemble of this dipeptide resembles that of the unblocked GAG model peptide with a pPII propensity of χ_{pPII} = 0.74. Investigation of the valine dipeptide and a comparison with the corresponding unblocked GVG tripeptide further reveals that the conformation of the target amino acid, in this case, valine, is the same in both model systems. These results show that the terminal groups do not have a experimentally significant influences on the conformations of nonterminal residues in unblocked peptides.

Results of MD simulations on cationic and zwitterionic AAA show that these peptides share similar Ramachadran plots. Both protonation states of AAA have a relatively higher pPII content as compared to the AdP, corroborating our experimental findings. In addition, radial distribution functions derived by MD simulations indicate that the amide proton of the central residue in AAA is on average in a much closer proximity water molecules, which may explain the higher enthalpic gains and stabilization of the pPII conformation for AAA relative to the AdP. We have shown that the hydration shell around AdP is much less ordered than around AAA. Consequently, the pPII preference in AdP is diminished relative to that of AAA, effectively decreasing the activation barrier of the pPII-β transition. Indeed, favorable backbone-solvent interactions in aqueous solution have been cited numerous times in literature as the primary source for stabilization of the pPII conformation.[8,20,41,49,56,61] We thus hypothesize that the choice of water model in MD simulations is instrumental for the reproduction of the experimentally observed conformational propensities in small peptides. In particular, polarizable water models and force field may prove critical in this regard.[43]

Recent efforts directed toward defining a pPII propensity scale in various host−guest peptides are part of the broader goal to establish a physical basis for the experimentally observed pPII preference in unfolded states. As such, the current study was directed toward determining whether there was any appreciable difference in the conformational ensemble upon protonation/deprotonation of terminal groups in short unblocked peptides. The findings reported herein for AAA do not indicate any difference in this regard. Further, since the blocked forms of amino acids show remarkable similarity to the unblocked GxG peptides, we conclude that these are both suitable model systems for studying the unfolded states and the pPII preference specifically.

■ ASSOCIATED CONTENT

Supporting Information

Theoretical and experimental amide I′ profiles of GAG and GVG, the experimentally determined Ramachandran plot of AdP, the $\Delta\varepsilon_{max}(T)$ graphs as well as the (φ, ψ)-time evolution and transition statistics obtained from MD simulations. This material is available free of charge via the Internet at http://pubs.acs.org.

■ AUTHOR INFORMATION

Corresponding Author

*Phone: 215-895-2268. Fax: 215-895-1265. E-mail: rschweitzer-stenner@drexel.edu.

Notes

The authors declare no competing financial interest.

■ ACKNOWLEDGMENTS

This research was supported by an NSF grant (Chem 0804492), and an REU supplement (Chem 0939972) to R.S.S. and by an NIH grant (AG027818) to B.U. This work used the Extreme Science and Engineering Discovery Environment (XSEDE), which is supported by National Science Foundation grant number PHYS100030 (B.U.).

■ REFERENCES

(1) Shi, Z.; Olson, C. A.; Rose, G. D.; Baldwin, R. L.; Kallenbach, N. R. Polyproline Ii Structure in a Sequence of Seven Alanine Residues. *Proc. Natl. Acad. Sci. U.S.A.* **2002**, *99*, 9190−9195.

(2) Chen, K.; Liu, Z.; Kallenbach, N. R. The Polyproline Ii Conformation in Short Alanine Peptides Is Non Cooperative. *Proc. Natl. Acad. Sci. U.S.A.* **2004**, *101*, 15352−15357.

(3) Ding, L.; Chen, K.; Santini, P. A.; Shi, Z.; Kallenbach, N. R. The Pentapeptide Ggagg Has Pii Conformation. *J. Am. Chem. Soc.* **2003**, *125*, 8092−8093.

(4) Shi, Z.; Shen, K.; Liu, Z.; Kallenbach, N. R. Conformation in the Backbone in Unfolded Proteins. *Chem. Rev.* **2006**, *106*, 1877−1897.

(5) Woutersen, S.; Hamm, P. Structure Determination of Trialanine in Water Using Polarized Sensitive Two-Dimensional Vibrational Spectroscopy. *J. Phys. Chem. B* **2000**, *104*, 11316−11320.

(6) Woutersen, S.; Hamm, P. Isotope-Edited Two-Dimensional Vibrational Spectroscopy of Trialanine in Aqueous Solution. *J. Chem. Phys.* **2001**, *114*, 2727−2737.

(7) Woutersen, S.; Pfister, R.; Hamm, P.; Mu, Y.; Kosov, D. S.; Stock, G. Peptide Conformational Heterogeneity Revealed from Nonlinear Vibrational Spectroscopy and Molecular-Dynamics Simulations. *J. Chem. Phys.* **2002**, *117*, 6833−6840.

(8) Han, W.-G.; Jakanen, K. J.; Elstner, M.; Suhai, S. Theoretical Study of Aqueous N-Acetyl-L-Alanine N-Methylamide: Structures and Raman, Vcd, and Roa Spectra. *J. Phys. Chem. B* **1998**, *102*, 2587−2602.

(9) Eker, F.; Griebenow, K.; Cao, X.; Nafie, L.; Schweitzer-Stenner, R. Preferred Peptide Backbone Conformations in the Unfolded State Revealed by the Structure Analysis of Alanine-Based (AXA) Tripeptides in Aqueous Solution. *Proc. Natl. Acad. Sci. U.S.A.* **2004**, *101*, 10054−10059.

(10) Hagarman, A.; Measey, T. J.; Mathieu, D.; Schwalbe, H.; Schweitzer-Stenner, R. Intrinsic Propensities of Amino Acid Residues in GxG Peptides Inferred from Amide I Band Profiles and Nmr Scalar Coupling Constants. *J. Am. Chem. Soc.* **2010**, *132*, 540−551.

(11) Hagarman, A.; Mathieu, D.; Toal, S.; Measey, T. J.; Schwalbe, H.; Schweitzer-Stenner, R. Amino Acids with Hydrogen-Bonding Side Chains Have an Intrinsic Propensity to Sample Various Turn Conformations in Aqueous Solution. *Chem.—Eur. J.* **2011**, *17*, 6789−6797.

(12) Schweitzer-Stenner, R. Conformational Propensities and Residual Structures in Unfolded Peptides and Proteins. *Mol. BioSyst.* **2012**, *8*, 122−133.

(13) Grdadolnik, J.; Mohacek-Grosev, V.; Baldwin, R. L.; Avbelj, F. Populations of the Three Makor Backbone Conformations in 19 Amino Acid Dipeptides. *Proc. Natl. Acad. Sci. U.S.A.* **2011**, *108*, 1794−1798.
(14) Poon, C. D.; Samulsi, E. T.; Weise, C. F.; Weisshaar, J. C. Do Bridging Water Molecules Dictate the Structure of a Model Dipeptide in Aqueous Solution? *J. Am. Chem. Soc.* **2000**, *122*, 5612−5613.
(15) Weise, C. F.; Weisshaar, J. C. Conformational Analysis of Alanine Dipeptide from Dipolar Couplings in a Water-Based Liquid Crystal. *J. Phys. Chem. B* **2003**, *107*, 3265−3277.
(16) Scholtz, J. M.; Marqusee, S.; Baldwin, R. L.; York, E. J.; Stewart, J. M.; Santoro, M.; W., B. D. Calorimetric Determination of the Enthalpy Change for the Alpha-Helix to Coil Transition of an Alanine Peptide in Water. *Proc. Natl. Acad. Sci. U.S.A.* **1991**, *88*, 2854−2860.
(17) Tanford, C. Protein Denaturation. *Adv. Prot. Chem.* **1968**, *23*, 121−282.
(18) Ramachandran, G. N.; Ramachandran, C.; Sasisekharan, V. Stereochemistry of Polypeptide Chain Configurations. *J. Mol. Biol.* **1963**, *7*, 95−99.
(19) Brant, D. A.; Flory, P. J. J. The Configuration of Random Polypeptide Chains. Ii. Theory. *J. Am. Chem. Soc.* **1965**, *87*, 2791−2800.
(20) Garcia, A. E. Characterization of Non-Alpha Conformations in Ala Peptides. *Polymer* **2004**, *120*, 885−890.
(21) Gnanakaran, S.; Garcia, A. E. Validation of an All-Atom Protein Force Field: From Dipeptides to Larger Peptides. *J. Phys. Chem. B* **2003**, *107*, 12555−12557.
(22) DeBartolo, J.; Jha, A.; Freed, K., F.; Sosnick, T. R., Local Backbone Preferences and Nearest Neighbor Effects in the Unfolded and Native States. In *Proteins and Peptides. Folding, Misfolding and Unfolding*; Schweitzer-Stenner, R., Ed.; Wiley & Sons: Chichester, 2012; pp 79−98.
(23) Jha, A. K.; Colubri, A.; Zaman, M. H.; Koide, S.; Sosnick, T. R.; Freed, K. F. Helix, Sheet and Polyproline Ii Frequencies and Strong Nearest Neighbor Effects in a Restricted Coil Library. *Biochemistry* **2005**, *44*, 9691−9702.
(24) Pizanelli, S.; Forte, C.; Monti, S.; Zandomeneghi, G.; Hagarman, A.; Measey, T. J.; Schweitzer-Stenner, R. Conformation of Phenylalanine in the Trpeptides AFA and GFG Probed by Combining MD Simulations with NMR, FTIR, Polarized Raman and VCD Spectroscopy. *J. Phys. Chem. B* **2010**, *114*, 3965−3978.
(25) Duitch, L.; Toal, S.; Measey, T. J.; Schweitzer-Stenner, R. Triaspartate: A Model System for Conformationally Flexible DDD Motifs in Proteins. *J. Phys. Chem. B* **2012**, *116*, 5160−5171.
(26) Verbaro, D.; Mathieu, D.; Toal, S. E.; Schwalbe, H.; Schweitzer-Stenner, R. Inoized Trilysine: A Model System for Understanding the Nonrandom Structure of Poly-L-Lysine and Lysine-Containing Motifs in Proteins. *J. Phys. Chem. B.* **2012**, *116*, 8084−8094.
(27) He, L.; Navarro, A. E.; Shi, Z.; Kallenbach, N. R. End Effects Influence Short Model Peptide Conformation. *J. Am. Chem. Soc.* **2011**, *134*, 1571−1576.
(28) Li, W.; Qin, M.; Tie, Z.; Wang, W. Effects of Solvents on the Intrinsic Propensity of Peptide Backbone Conformations. *Phys. Rev. E* **2011**, *84*, 041933.
(29) Ioannou, F.; Archontis, G.; Leontidis, E. Specific Interactions of Sodium Salts with Alanine Dipeptide and Tetrapeptide in Water: Insights from Molecular Dynamics. *J. Phys. Chem. B* **2011**, *115*, 13389−13400.
(30) Feig, M. Is Alanine Dipeptide a Good Model for Representing the Torsional Preferences of Protein Backbones. *J. Chem. Theory Comput.* **2008**, *4*, 1555−1564.
(31) Shi, Z.; Chen, K.; Liu, Z.; Ng, A.; Bracken, W. C.; Kallenbach, N. R. Polyproline Ii Propensities from GGXGG Peptides Reveal an Anticorrelation with β-Sheet Scales. *Proc. Natl. Acad. Sci. U.S.A.* **2005**, *102*, 17964−17968.
(32) Garcia-Pietro, F. F.; Galván, I. F.; Aguliar, M. A.; Martin, M. E. Study on the Conformational Equilibrium of the Alanine Dipeptide in Water Solution by Using the Averaged Solvent Electrostatic Potential from Molecular Dynamics Methodology. *J. Chem. Phys.* **2011**, *135*, 194502.
(33) Kim, Y. S.; Wang, J.; Hochstrasser, R. M. Two-Dimensional Infrared Spectroscopy of the Alanine Dipeptide in Aqueous Solution. *J. Phys. Chem. B* **2005**, *109*, 7511−7521.
(34) Avbelj, F.; Gradolnik, S. G.; Grdadolnik, J.; Baldwin, R. L. Intrinsic Backbone Preferences Are Fully Present in Blocked Amino Acids. *Proc. Natl. Acad. Sci. U.S.A.* **2006**, *103*, 1272−1277.
(35) Grdadolnik, J.; Grdadolnik, S. G.; Avbelj, F. Determination of Conformational Preferences of Dipeptides Using Vibrational Spectroscopy. *J. Phys. Chem. B* **2008**, *112*, 2712−2718.
(36) Ishizuka, R.; Huber, G. A.; McCammon, J. A. Solvation Effect on the Conformation of Alanine Dipeptide: Integral Equation Approach. *J. Phys. Chem. Lett.* **2011**, *1*, 2279−2283.
(37) Cruz, V.; Ramos, j.; Martinez-Salazar, J. Water-Mediated Conformations of the Alanine Dipeptide as Revealed by Distributed Umbrella Sampling Simulations, Quantum Mechanics Based Calculations, and Experimental Data. *J. Phys. Chem. B* **2011**, *115*, 4880−4886.
(38) Jansen, T. C.; Knoester, J. Nonadiabatic Effects in the Two-Dimensional Infrared Spectra of Peptides: Application to Alanine Dipeptide. *J. Phys. Chem. B.* **2006**, *110*, 22910−22916.
(39) Xu, C.; Wang, J.; Liu, H. A Hamiltonian Replica Exchange Approach and Its Application to the Study of Side-Chain Type and Neighbor Effects on Peptide Backbone Conformations. *J. Chem. Theory Comput.* **2008**, *4*, 1348−1359.
(40) Han, C.; Wang, J. Influence of an Unnatural Amino Acid Side Chain on the Conformational Dynamics of Peptides. *Chem. Phys. Chem.* **2012**, *13*, 1522−1534.
(41) Drozdov, A. N.; Grossfield, A.; Pappu, R. V. Role of Solvent in Determining Conformational Preferences of Alanine Dipeptide in Water. *J. Am. Chem. Soc.* **2004**, *126*, 2574−2581.
(42) Gaigeot, M.-P. Infrared Spectroscopy of the Alanine Dipeptide Analog in Liquid Water with DFT-MD. Direct Evidence for PII/β Conformations. *Phys. Chem. Phys. Chem.* **2010**, *12*, 10198−10209.
(43) Kwac, K.; Lee, K.-K.; Han, J. B.; Oh, K.-I.; Cho, M. Classical and Quantum Mechanical/Molecular Mechanical Molecular Dynamics Simulations of Alanine Dipeptide in Water: Comparison with IR and Vibrational Circular Dichroism Spectra. *J. Chem. Phys.* **2008**, *128*, 105106.
(44) Oh, K.-I.; Jung, Y.-S.; Hwang, G.-S.; Cho, M. Conformational Distributions of Denaturated and Unstructured Proteins Are Similar to Those of 20 × 20 Blocked Dipeptides. *J. Biomol. NMR* **2012**, *53*, 25−41.
(45) Oh, K.-I.; Lee, K.-K.; Park, E.-K.; Jung, Y.-S.; Hwang, G.-S.; Cho, M. A Comprehensive Library of Blocked Dipeptides Reveals Intrinsic Backbone Conformational Propensities of Unfolded Proteins. *Proteins Struct. Funct. Genet.* **2012**, *80*, 977−990.
(46) Gorbunov, R. D.; Kosov, D. S.; Stock, G. *Ab Initio*-Based Exciton Model of Amide I Vibrations in Peptides: Definition, Conformational Dependence and Transferrability. *J. Chem. Phys.* **2005**, *122*, 224904−224915.
(47) Gorbunov, R. D.; Nguyen, P. H.; Kobus, M.; Stock, G. Quantum-Classical Description of the Amide I Vibrational Spectrum of Trialanine. *J. Chem. Phys.* **2007**, *126*, 054509.
(48) Eker, F.; Cao, X.; Nafie, L.; Schweitzer-Stenner, R. Tripeptides Adopt Stable Structures in Water. A Combined Polarized Visible Raman, FTIR and VCD Spectroscopy Study. *J. Am. Chem. Soc.* **2002**, *124*, 14330−14341.
(49) Eker, F.; Cao, X.; Nafie, L.; Griebenow, K.; Schweitzer-Stenner, R. The Structure of Alanine Based Tripeptides in Water and Dimethyl Sulfoxide Probed by Vibrational Spectroscopy. *J. Phys. Chem. B* **2003**, *107*, 358−365.
(50) Graf, J.; Nguyen, P. H.; Stock, G.; Schwalbe, H. Structure and Dynamics of the Homologous Series of Alanine Peptides: A Joint Molecular Dynamics/Nmr Study. *J. Am. Chem. Soc.* **2007**, *129*, 1179−1189.

(51) Avbelj, F.; Baldwin, R. L. Role of Backbone Solvation and Electrostatics in Generating Preferred Peptide Backbone Conformations: Distributions of Phi. *Proc. Natl. Acad. Sci. U.S.A.* **2003**, *100*, 5742−5747.
(52) Avbelj, F.; Baldwin, R. L. Origin of the Neighboring Residue Effect on Peptide Backbone Conformation. *Proc. Natl. Acad. Sci. U.S.A.* **2004**, *101*, 19067−10972.
(53) Duan, Y.; et al. A Point-Charge Force Field for Molecular Mechanics Simulations of Protein Based on Condensed-Phase Quantum Mechanical Calculations. *J. Comput. Chem.* **2003**, *24*, 1999−2012.
(54) Zagrovic, B.; Lipfert, J.; Sorin, E. J.; Millett, I. S.; van Gunsteren, W. F.; Doniach, S.; Pande, V. S. Unusual Compactness of a Polyproline Ii Structure. *Proc. Natl. Acad. Sci. U.S.A.* **2005**, *102*, 11698−11703.
(55) Best, R. B.; Buchete, N. V.; Hummer, G. Are Current Molecular Dynamics Force Fields Too Helical? *Biophys. J.* **2008**, *95*, L07−L09.
(56) Gnanakaran, S.; Garcia, A. E. Helix-Coil Transition of Alanine Peptides in Water: Force Field Dependence on the Folded and Unfolded Structures. *Proteins* **2005**, *59*, 773−782.
(57) Mu, Y.; Kosov, D. S.; Stock, G. Conformational Dynamics of Trialanine in Water. 2. Comparison of Amber, Charmm, Gromos, and Opls Force Fields to NMR and Infrared Experiments. *J. Phys. Chem. B* **2003**, *107*, 5064−5073.
(58) Mu, Y.; Stock, G. Conformational Dynamics of Trialanine in Water: A Water Dynamics Study. *J. Phys. Chem. B* **2002**, *106*, 5294−5301.
(59) Glasoe, P. K.; Long, F. A. Use of Glass Electrodes to Measure Acidities in Deuterium Oxide. *J. Phys. Chem.* **1960**, *64*, 188−190.
(60) Jentzen, W.; Unger, E.; Karvounis, G.; Shelnutt, J. A.; Dreybrodt, W.; Schweitzer-Stenner, R. Conformational Properties of Nickel(Ii) Octaethylporphyrin in Solution. 1. Resonance Excitation Profiles and Temperature Dependence of Structure-Sensitive Raman Lines. *J. Phys. Chem.* **1995**, *100*, 14184−14191.
(61) Toal, S.; Omidi, A.; Schweitzer-Stenner, R. Conformational Changes of Trialanine Induced by Direct Interactions between Alanine Residues and Alcohols in Binary Mixtures of Water with Glycerol and Ethanol. *J. Am. Chem. Soc.* **2011**, *133*, 12728−12739.
(62) Kaminski, G. A.; Friesner, R. A.; Tirado-Rives, J.; Jorgensen, W. L. Evaluation and Reparametrization of the OPLS-AA Force Field for Proteins Via Comparison with Accurate Quantum Chemical Calculations on Peptides. *J. Phys. Chem. B* **2001**, *105*, 6474−6487.
(63) Jorgensen, W. L.; Chandrasekhar, J.; Madura, J. D.; Impey, R. W.; Klein, M. L. Comparison of Simple Potential Functions for Simulating Liquid Water. *J. Chem. Phys.* **1983**, *79*, 926−935.
(64) Berendsen, H. J. C.; Grigera, J. R.; Straatsma, T. P. The Missing Term in Effective Pair Potentials. *J. Phys. Chem.* **1987**, *91*, 6269−6271.
(65) Horn, H. W.; Swope, W. C.; Pitera, J. W.; Madura, J. D.; Dick, T. J.; Hura, G. L.; Head-Gordon, T. Development of an Improved Four-Site Water Model for Biomolecular Simulations: TIP4P-EW. *J. Chem. Phys.* **2004**, *120*, 9665−9678.
(66) Schweitzer-Stenner, R. Advances in Vibrational Spectroscopy as a Sensitive Probe of Peptide and Protein Structure. A Critical Review. *Vibr. Spectrosc.* **2006**, *42*, 98−117.
(67) Krimm, S.; Bandekar, J. Vibrational Spectroscopy of Peptides and Proteins. *Adv. Protein Chem.* **1986**, *38*, 181.
(68) Chen, X. G.; Schweitzer-Stenner, R.; Mirkin, N. G.; Krimm, S.; Asher, S. A. N-Methylacetamide and Its Hydrogen-Bonded Water Molecules Are Vibrationally Coupled. *J. Am. Chem. Soc.* **1994**, *116*, 11141−11142.
(69) Sieler, G.; Schweitzer-Stenner, R. The Amide I Mode of Peptides in Aqueous Solution Involves Vibrational Coupling between the Peptide Group and Water Molecules of the Hydration Shell. *J. Am. Chem. Soc.* **1997**, *119*, 1720−1726.
(70) Sieler, G.; Schweitzer-Stenner, R.; Holtz, J. S. W.; Pajcini, V.; Asher, S. A. Different Conformers and Protonation States of Dipeptides Probed by Polarized Raman, UV-Resonance Raman, and FTIR Spectroscopy. *J. Phys. Chem. B* **1999**, *103*, 372−384.
(71) Schweitzer-Stenner, R.; Eker, F.; Huang, Q.; Griebenow, K.; Mroz, P. A.; Kozlowski, P. M. Structure Analysis of Dipeptides in Water by Exploring and Utilizing the Structural Sensitivity of Amide III by Polarized Visible Raman, FTIR-Spectroscopy and DFT Based Normal Coordinate Analysis. *J. Phys. Chem. B* **2002**, *106*, 4294−4304.
(72) Schweitzer-Stenner, R. Dihedral Angles of Tripeptides in Solution Determined by Polarized Raman and FTIR Spectroscopy. *Biophys. J.* **2002**, *83*, 523−332.
(73) Schweitzer-Stenner, R. Distribution of Conformations Sampled by the Central Amino Acid Residue in Tripeptides Inferred from Amide I Band Profiles and Nmr Scalar Coupling Constants. *J. Phys. Chem. B* **2009**, *113*, 2922−2932.
(74) Schweitzer-Stenner, R. Secondary Structure Analysis of Polypeptides Based on an Excitonic Coupling Model to Describe the Band Profile of Amide I′ of IR, Raman, and Vibrational Circular Dichroism Spectra. *J. Phys. Chem. B* **2004**, *108*, 16965−16975.
(75) Karplus, M. Theoretical Calculation Links NMR Coupling Constant to Molecular Geometry. *J. Chem. Phys.* **1959**, *30*, 11−15.
(76) Schweitzer-Stenner, R.; Eker, F.; Huang, Q.; Griebenow, K. Dihesral Angles of Trialanine in D_2O Determined by Combining FTIR and Polarized Visible Raman Spectroscopy. *J. Am. Chem. Soc.* **2001**, *123*, 9628−9633.
(77) Schweitzer-Stenner, R.; Measey, T. The Alanine-Rich XAO Peptide Adopts a Heterogeneous Population, Including Turn-Like and PPII Conformations. *Proc. Natl. Acad. Sci. U.S.A.* **2007**, *104*, 6649−6654.
(78) Schweitzer-Stenner, R.; Measey, T.; Kakalis, L.; Jordan, F.; Pizzanelli, S.; Forte, C.; Griebenow, K. Conformations of Alanine-Based Peptides in Water Probed by FTIR, Raman, Vibrational Circular Dichroism, Electronic Circular Dichroism, and NMR Spectroscopy. *Biochemistry* **2007**, *46*, 1587−1596.
(79) Schweitzer-Stenner, R.; Hagarman, A.; Toal, S.; Mathieu, D.; Schwalbe, H. Disorder and Order in Unfolded Peptides and Proteins. A View Derived from Tripeptide Conformational Analysis.I. Tripeptides with Long and Predominantly Hydrophobic Side Chains. *Proteins: Struct., Funct. Genet.* **2012**, DOI: 10.1002/prot.24225.
(80) Oh, K.-I.; Lee, K.-K.; Park, E. K.; Kwang, G. S.; Cho, M. Circular Dichroism Eigenspectra of Polyproline II and B-Strand Conformers of Trialanine in Water: Singular Value Decomposition Analysis. *Chirality* **2010**, *22*, E186−E201.
(81) Jansen, T. C.; Dijkstra, A.; Watson, T. M.; Hirst, J. D.; Knoester, J. Modelling of the Amide I Bands of Small Peptides. *J. Chem. Phys.* **2006**, *125*, 044132.
(82) Schweitzer-Stenner, R.; Gonzales, W.; Bourne, J. T.; Feng, J. A.; Marshall, G. A. Conformational Manifold of a-Aminoisobutyric Acid (Aib) Containing Alanine-Based Tripeptides in Aqueous Solution Explored by Vibrational Spectroscopy, Electronic Circular Dichroism Spectroscopy, and Molecular Dynamics Simulations. *J. Am. Chem. Soc.* **2007**, *129*, 13095−13109.
(83) Rybka, K.; Toal, S.; Verbaro, D.; Mathieu, D.; Schwalbe, H. Disorder and Order in Unfolded Peptides and Proteins. A View Derived from Tripeptide Conformational Analysis II. Tripeptides with Short Side Chains Populating Asx and β-type Like Turn Conformations. *Proteins: Struct., Funct. Genet.* **2012**, DOI: 10.1002/prot.24226.
(84) Eker, F.; Griebenow, K.; Schweitzer-Stenner, R. Stable Conformations of Tripeptides in Aqueous Solution Studied by UV Circular Dichroism Spectroscopy. *J. Am. Chem. Soc.* **2003**, *125*, 8178−8185.
(85) Woody, R. W. Circular Dichroism Spectrum of Peptides in the Poly(Pro)II Conformation. *J. Am. Chem. Soc.* **2009**, *131*, 8234−8245.
(86) Chen, K.; Liu, Z.; Zhou, C.; Shi, Z.; Kallenbach, N. R. Neighbor Effect on pPII Conformation in Alanine Peptides. *J. Am. Chem. Soc.* **2005**, *127*, 10146−10147.
(87) Yang, W. Y.; Larios, E.; Gruebele, M. On the Extended β-Conformation of Polypeptides at High Temperatures. *J. Am. Chem. Soc.* **2003**, *125*, 16220−16227.
(88) Pajcini, V.; Chen, X. G.; Bormett, R. W.; Geib, S. J.; Li, P.; Asher, S. A.; Lidiak, E. G. Glycylglycine $\pi\rightarrow\pi^*$ and Charge Transfer Transition Moment Orientations: Near Resonance Raman Single Crystal Measurements. *J. Am. Chem. Soc.* **1996**, *118*, 9716−9726.

(89) Dragomir, I.; Measey, T. J.; Hagarman, A. M.; Schweitzer-Stenner, R. Environment-Controlled Interchromophore Charge Transfer Transitions in Dipeptides Probed by UV Absorption and Electronic Circular Dichroism Spectroscopy. *J. Phys. Chem. B* **2006**, *110*, 13235−13241.
(90) Measey, T.; Schweitzer-Stenner, R. The Conformations Adopted by the Octamer Peptide $(AAKA)_2$ in Aqueous Solution Probed by FTIR and Polarized Raman Spectroscopy. *J. Raman Spectrosc.* **2006**, *37*, 248−254.
(91) Kaur, H.; Sasidhar, Y. U. For the Sequence YGKQ, the Turn and Extended Conformational Forms Are Separated by Small Barriers and the Turn Propensity Persists Even at High Temperatures: Implications for Protein Folding. *J. Phys. Chem. B* **2012**, *116*, 3850−3860.
(92) Duan, Y.; et al. A Point-Charge Force Field for Molecular Mechanics Simulations of Proteins Based on Condensed-Phase Quantum Mechanical Calculations. *J. Comput. Chem.* **2003**, *24*, 1999−2012.
(93) Nerenberg, P.; Head-Gordon, T. Optimizing Protein-Solvent Force Fields to Reproduce Conformational Preferences of Model Peptides. *J. Chem. Theory Comp.* **2011**, *4*, 1220−1230.
(94) Best, R. B.; Hummer, G. Optimized Molecular Dynamics Force Fields Applied to the Helix-Coil Transition of Polypeptides. *J. Phys. Chem. B* **2009**, *113*, 9004−9015.
(95) Maladier-Jugroot, C.; Bowron, D. T.; Soper, a. K.; Johnson, M. E.; Head-Gordon, T. Structure and Water Dynamics of Aqueous Peptide Solutions in the Present of Co-Solvents. *Phys. Chem. Chem. Phys.* **2010**, *12*, 382−292.
(96) Kim, S.; Hochstrasser, R. M. The 2D IR Responses of Amide and Carbonyl Modes in Water Cannot Be Described by Gaussian Frequency Fluctuations. *J. Phys. Chem. B* **2007**, *111*, 9697−9701.